

Emerging Drug Interaction Prediction Enabled by Flow-based Graph Neural Network with Biomedical Network

Yongqi Zhang^a, Quanming Yao ^{*b}, Ling Yue^b, Xian Wu^c, Ziheng
Zhang^c, Zhenxi Lin^c, and Yefeng Zheng^c

^a*4Paradigm Inc., Beijing, China*

^b*Department of Electronic Engineering, Tsinghua University, Beijing, China*

^c*Tencent Jarvis Lab, Shenzhen, China*

Abstract

Accurately predicting drug-drug interactions (DDI) for emerging drugs, which offer possibilities for treating and alleviating diseases, with computational methods can improve patient care and contribute to efficient drug development. However, many existing computational methods require large amounts of known DDI information, which is scarce for emerging drugs. In this paper, we propose EmerGNN, a graph neural network (GNN) that can effectively predict interactions for emerging drugs by leveraging the rich information in biomedical networks. EmerGNN learns pairwise representations of drugs by extracting the paths between drug pairs, propagating information from one drug to the other, and incorporating the relevant biomedical concepts on the paths. The different edges on the biomedical network are weighted to indicate the relevance for the target DDI prediction. Overall, EmerGNN has higher accuracy than existing approaches in predicting interactions for emerging drugs and can identify the most relevant information on the biomedical network.

*Corresponding author: qyaoaa@tsinghua.edu.cn

1 Introduction

Science advancements and regulatory changes have led to the development of numerous emerging drugs worldwide, particularly for rare, severe, or life-threatening illnesses [1, 2]. These drugs are novel substances with unknown or unpredictable risks, as they have not been extensively regulated or used before. For instance, although hundreds of COVID-19 drugs have been developed, only six have been recommended by the FDA as of Oct 2023, such as dexamethasone and hydrocortisone. Clinical deployment of new drugs is cautious and slow, making it crucial to identify drug-drug interactions (DDIs) for emerging drugs. To speed up the discovery of potential DDIs, computational techniques, particularly machine learning approaches, have been developed [3–6]. However, with limited clinical trial information, unexpected polypharmacy or side effects can be severe and difficult to detect [7, 8].

Early DDI prediction methods used fingerprints [9] or hand-designed features [4, 10] to indicate interactions based on drug properties. Although these methods can work directly on emerging drugs in a cold-start setting [10, 11], they can lack expressiveness and ignore the mutual information between drugs. DDI facts can naturally be represented as a graph where nodes represent drugs and edges represent interactions between a pair of drugs. Graph learning methods can learn drug embeddings for prediction [12], but they rely on historical interactions, thus cannot address the problem of scarce interaction data for emerging drugs.

Incorporating large biomedical networks as side information for DDI prediction is an alternative to learning solely from DDI interactions [5, 6, 13–17]. These biomedical networks, such as HetioNet [18], organize facts into a directed multi-relational graph, recording relationships between biomedical concepts, such as genes, diseases, and drugs. Tanvir et. al. used hand-designed meta-paths from the biomedical network [5], while Karim et. al. learned embeddings from the network and used a deep network to do DDI prediction [14]. Graph neural networks [19, 20] can obtain expressive node embeddings by aggregating topological structure and drug embeddings, but existing methods [6, 13, 15–17] do not specially consider emerging drugs, leading to poor performance in predicting DDIs for them.

Here, we propose to use large biomedical network to predict DDI for emerging drugs by learning from the biomedical concepts connecting target drugs pairs. Although emerging drugs may not have sufficient interactions in the DDI network, they often share the same biochemical concepts used in the drug development with existing drugs, such as targeted genes or diseases. Therefore, we exploit related paths from the biomedical networks for given drug pairs. However, properly utilizing these networks can be challenging as they are not developed for emerging drugs, and the mismatch of objectives can lead machine learning models to learn distracting knowledge.

To accurately and interpretable predict DDI for emerging drugs, we introduce EmerGNN, a GNN method that learns pair-wise drug representations by integrating the biomedical entities and relations connecting them. A flow-

based GNN architecture extracts paths connecting drug pairs, traces from an emerging drug to an existing drug, and integrates information of the biomedical concepts along the paths. This approach utilizes shared information in both biomedical and interaction networks. To extract relevant information, we weight different types of relations on the biomedical network, and edges with larger weights on the paths are helpful for interpretation. Compared with other GNN-based methods, EmerGNN propagates on the local subgraph around the drug pair to be predicted and better discovers directional information flow within the biomedical network. In summary, our main contributions are as follows:

- Building upon a biomedical network, we develop an effective deep learning method that predicts interactions for emerging drugs accurately.
- We propose EmerGNN, a GNN-based method that learns pair-wise representations of drug pairs to predict DDIs for emerging drugs by integrating the relevant biomedical concepts connecting them.
- Extensive experiments show that EmerGNN is effective in predicting interactions for emerging drugs. The learned concepts on the biomedical network are interpretable.
- EmerGNN’s strong prediction ability has the potential to clinically improve patient care and contribute to more efficient drug development processes.

2 Results

EmerGNN: encoding pair-wise representations with flow-based GNN for emerging drugs. We focus on two DDI prediction task settings for emerging drugs [10, 11, 21] (Fig. 1a, Method): S1 setting, determining the interaction type between an emerging drug and an existing drug, and S2 setting, determining the interaction type between two emerging drugs. To connect emerging and existing drugs, we use a large biomedical network HetioNet [18], which contains entities and relations related to biomedical concepts. We assume that all the emerging drugs are connected to entities in the biomedical network, allowing us to infer their properties from existing drugs and the biomedical network.

Given the DDI network and biomedical network (Fig. 1a), we firstly integrate the two networks to enable communication between existing and emerging drugs connected by biomedical concepts, such as proteins, diseases or other drugs, and then add inverse edges by introducing inverse types for each relation and interaction type. The two steps generate an augmented network where the drugs and biomedical entities can communicate better (Fig. 1b). For a target drug pair to be predicted (for example an emerging drug u and an existing drug v), we extract all the paths with length no longer than L between them, and combine the paths to form a path-based subgraph $\mathcal{G}_{u,v}^L$ (Fig. 1c). The value of L is a hyper-parameter to be tuned (Supplementary Table 2). A flow-based GNN

$g(\cdot; \theta)$ with parameters θ (Fig. 1d) is applied on $\mathcal{G}_{u,v}^L$ to trace drug features $\mathbf{h}_{u,u}^0 = \mathbf{f}_u$ (like fingerprints) along the biomedical edges and integrate essential information along the path. In each iteration ℓ , the GNN flows to drug-specific entities that are ℓ -steps away from drug u and $(L - \ell)$ -steps away from drug v in the augmented network. An attention mechanism is applied on the edges in $\mathcal{G}_{u,v}^L$ to adjust their importance. The GNN iterates L steps to return the pair-wise representation $\mathbf{h}_{u,v}^{(L)}$. Finally, $\mathbf{h}_{u,v}^{(L)}$ is fed to a linear classifier $p(\cdot)$ to predict the interaction type between u and v (Fig. 1e).

Comparison of EmerGNN to baseline methods in DDI prediction.

Two public datasets DrugBank [22] and TWOSIDES [23] are used. The original drug set is split into three parts with a ratio of 7:1:2 for training, validation, and testing (Method). The drugs in validation and testing sets are considered emerging drugs for validation and testing, respectively. For the DrugBank dataset, there is at most one interaction type between any drug pair, and the task is to predict the exact type in a multi-type classification setting. Macro F1-score, Accuracy, and Cohen’s Kappa [24] are used as performance metrics, with F1-score as the primary metric. For TWOSIDES dataset, there may be multiple interaction types between a drug pair, and the task is to predict whether a pair of drugs will have a certain interaction type under a binary classification setting. PR-AUC, ROC-AUC and Accuracy are used to evaluate the performance, with PR-AUC being the primary metric.

In S1 setting, *Emb* type methods, particularly MSTE, poorly predict emerging drugs because their embeddings are not updated during training. KG-DDI performs better as it updates drug embeddings with information in the biomedical network. For *DF* methods, CSMDDI and STNN-DDI outperform MLP on DrugBank dataset with their designed training schemes in a cold-start setting, but they do not perform well on TWOSIDES with more interaction types. HIN-DDI outperforms MLP, indicating that graph features from biomedical network can benefit DDI prediction. Deep *GNN*-based methods may not perform better than *DF* methods on DrugBank since the GNN-based methods may not well capture the crucial property of similarity for emerging drug prediction (Fig. 3). CompGCN, Decagon and KGNN perform comparably due to their similar GNN architecture design. SumGNN constrains message passing in the enclosing subgraph between drug pairs, making information more focused. DeepLGF is the best GNN-based baseline by fusing information from multiple sources, taking the advantage of both drug features and graph features. EmerGNN significantly outperforms all compared methods as indicated by the small p-values under two-sided t-testing of statistical significance. First, by learning paths between emerging and existing drugs, it can capture the graph features, whose importance has been verified by the *GF* method HIN-DDI. Second, different from CompGCN, Decagon, KGNN, and DeepLGF, the importance of edges can be weighted such that it can implicitly learn the similarity properties (Fig. 3). Third, with the designed path-based subgraph and flow-based GNN architecture, EmerGNN captures more relevant information from the biomedical

network, thus outperforming **CompGCN** and **SumGNN** (Supplementary Figure 4) as well.

We evaluate the top-performing models in each type in the more challenging S2 setting (Table 1), where both drugs are new with sparser information. While **KG-DDI** and **DeepLGF** performed well in S1 setting, they struggled in S2 setting since they need to learn representations of both drugs effectively. Conversely, **CSMDDI** and **HIN-DDI** performed more consistently, with **CSMDDI** ranking second on DrugBank and **HIN-DDI** ranking second on TWOSIDES. This may be due to their simple models but effective features. In comparison, **EmerGNN** significantly outperforms all the baselines under two-sided t-testing of statistical significance by aggregating essential information from the biomedical network. Additionally, we provide results for the S0 setting (Supplementary Table 3), which predicts interactions between existing drugs. We thoroughly investigate why **EmerGNN** has superior performance for DDI prediction in the following results.

Analysis of the Computational complexity. Since **EmerGNN** learns pairwise representations for each drug pair, the computation complexity is higher than the other GNN-based methods. However, **EmerGNN** can achieve higher accuracy than other GNN-based methods in just a few hours, and longer training time has the potential to achieve even better performance (Fig. 2a-b). Among the baseline GNN methods, **Decagon** is the most efficient as it only uses information related to drug, protein and disease in the biomedical network. **SumGNN** and **EmerGNN** are slower than **Decagon** and **DeepLGF** as they need to learn specific subgraph representations for different drug pairs. Given that the clinical development of a typical innovative drug usually takes years [25], the computation time of **EmerGNN** is acceptable. We also compare the GPU memory footprint (Fig. 2c) and the number of parameters (Fig. 2d) of these GNN-based models. It is clear that **EmerGNN** is memory and parameter efficient. First, its subgraphs for DDI prediction are much smaller than the biomedical network (Supplementary Figure 1). Second, **EmerGNN** mainly relies on the biomedical concepts instead of the drugs’ embeddings to do predictions, resulting in a small number of parameters. In comparison, **DeepLGF** requires a large number of model parameters to learn embeddings from the biomedical network.

Analysis of drug interaction types in the learned subgraph. **EmerGNN** uses attention weights to measure the importance of edges in the subgraph for predicting DDI of the emerging drugs. Here, we analyze what is captured by the attention weights by checking correlations between predicted interaction types with interactions and relations in the path-based subgraphs (Fig. 3).

We firstly analyze the correlations between the interaction type i_{pred} to be predicted and interaction types obtained in the selected paths. The dominant diagonal elements in the heatmap (Fig. 3a) suggests that when predicting a target interaction i_{pred} for (u, v) , paths with larger attention weights in the subgraph $\mathcal{G}_{u,v}^L$ are likely to go through another drug (for instance u_1) that has interaction $i_1 = i_{\text{pred}}$ with the existing drug v . We suppose that these drugs

like u_1 may have similar properties as the emerging drug u . To demonstrate this point, we group these cases of drug pairs (u, u_1) as *Group 1* and other pairs (u, u_2) with a random drug u_2 as *Group 2*. The distributions of drug fingerprints similarities show that *Group 1* has a larger quantity of highly similar drug pairs (> 0.5) than *Group 2* (Fig. 3b), demonstrating the crucial role of similar drugs in predicting DDIs for emerging drugs, and our method can implicitly search for these drugs. Apart from the diagonal part, there exists strongly correlated pairs of interactions. This happens, for example, when the emerging drug u finds some connections with another drug u_3 whose intersection i_3 with the existing drug v is correlated with i_{pred} . In these cases, we find strongly correlated pairs like “increasing constipating activity” and “decreasing analgesic activity” (Fig. 3a, Supplementary Table 5), verified by Liu et al. [26].

We then analyze the biomedical relation types in the selected paths by visualizing correlations between the interaction to be predicted i_{pred} and biomedical relation types in the selected paths. There are a few relation types consistently selected when predicting different interaction types (Fig. 3c). In particular, the most frequent relation type is the drug resembling relation CrC, which again verifies the importance of similar drugs for emerging drug prediction. Other frequently selected types are related to diseases (CrD), genes (CbG), pharmacologic classes (PCiC) and side effects (CsSE). To analyze their importance, we compare the performance of **EmerGNN** with the full biomedical network, and networks with only top-1, top-3, or top-5 attended relations (the middle part of Fig. 3d). As a comparison, we randomly sample 10%, 30% and 50% edges from the biomedical performance and show the performance (the right part of Fig. 3d). Keeping the top-1, top-3 and top-5 relations in biomedical network can all lead to comparable performance as using a full network. However, the performance substantially deteriorates when edges are randomly dropped. These experiments show that EmerGNN selects important and relevant relations in the biomedical network for DDI prediction.

Case study on drug-pairs. We present cases of selected paths from subgraphs by selecting top ten paths between u and v based on the average of edges’ attention weights on each path (Fig. 4a-b). In the first case, there are interpretable paths supporting the target prediction (Supplementary Table 6). For example, there are paths connecting the two drugs through the binding protein Gene::1565 (CYP2D6), which is a P450 enzyme that plays a key role in drug metabolism [27]. Another path finds a similar drug DB00424 (Hyoscyamine) of DB00757 (Dolasetron) through the resemble relation (CrC), and concludes that DB06204 (Tapentadol) may potentially decrease the analgesic activity of DB00757 (Dolasetron) due to the correlation between constipating and analgesic activities (Fig. 3a). In the second case, we make similar observations (Supplementary Table 6). In particular, a path finds a similar drug DB00421 (Spironolactone) of DB00598 (Labetalol), which may decrease the vasoconstricting activity of DB00610 (Metaraminol), providing a hint that Labetalol may also decrease the vasoconstricting activity

of Metaraminol. Compared with the original subgraphs $\mathcal{G}_{u,v}^L$ which have tens of thousands of edges (Supplementary Figure 1), the learned subgraphs are much smaller and more relevant to the target prediction. More examples with detailed interpretations on the paths can support that EmerGNN finds important paths that indicate relevant interaction types and biomedical entities for emerging drug prediction (Supplementary Figure 5).

Next, we visualize the drug pair representations obtained by CompGCN, SumGNN and EmerGNN (Fig. 4c-e). As shown, the drug pairs with the same interaction are more densely gathered in EmerGNN than CompGCN and SumGNN. This means that the drug pair representations of EmerGNN can better separate the different interaction types. As a result, EmerGNN is able to learn better representations than the other GNN methods, like CompGCN and SumGNN.

Ablation studies. We compare the performance of top-performing models according to the frequency of interaction types to analyze the different models’ ability (Fig. 5a). EmerGNN outperforms the baselines in all frequencies. For the high frequency relations (1%~20%), all the methods, except for KG-DDI, have good performance. For extremely low frequency relations (81%~100%), all the methods work poorly. The performance of all methods deteriorates in general for relations with a lower frequency. However, the relative performance gain of EmerGNN tends to be larger, especially in the range of 61%~80%. These results indicate EmerGNN’s strengths in generalization and ability to extract essential information from the biomedical network for predicting rare drugs and interaction types.

The main experiments (Table 1) study the scenario of emerging drugs without any interaction to existing drugs. In practice, we may have a few known interactions between the emerging and existing drugs, often obtained from limited clinical trials. Hence, we analyze how different models perform if adding a few interactions for each emerging drug (Fig. 5b). We can see that the performance of shallow models such as CSMDDI and HIN-DNN does not change much since the features they use are unchanged. However, methods learning drug embeddings, such as KG-DDI and DeepLGF, enjoy more substantial improvement when additional knowledge is provided. In comparison, EmerGNN has increased performance with more interactions added and is still the best over all the compared methods.

The value of L determines the maximum number of hops of neighboring entities that the GNN-based models can visit. We study the impact of changing the length L for these methods (Fig. 5c). The performance of Decagon and DeepLGF gets worse when L gets larger. Considering that Decagon and DeepLGF work on the full biomedical network, too many irrelevant information will be involved in the representation learning, leading to worse performance. DeepLGF runs out-of-memory when $L \geq 3$. For SumGNN and EmerGNN, $L = 1$ performs the worst as the information is hard to be passed from the emerging drug to the existing drug. SumGNN can leverage the drug features for prediction, thus outperforms Decagon. In comparison, EmerGNN benefits much from the

relevant information on the biomedical network when L increases from 1 to 3. However, the performance will decrease when $L > 3$. Intuitively, the path-based subgraph will contain too much irrelevant information when the length gets longer, increasing the learning difficulty. Hence, a moderate number of path length with $L = 3$ is optimal for EmerGNN, considering both the effectiveness and computation efficiency.

We conduct experiments to analyze the main techniques in designing in EmerGNN (Fig. 5d). First, we evaluate the performance of using undirected edges without introducing the inverse edges (denoted as Undirected edges w.o. inverse). It is clear that using undirected edges has negative effect as the directional information on the biomedical network is lost. Then, we design a variant, that learns a subgraph representation as SumGNN upon $\mathcal{G}_{u,v}^L$ (denoted as Subgraph representation), and another variant that only learns on the uni-directional computing (Method) from direction u to v without considering the direction from v to u (denoted as Uni-directional pair-wise representation). Comparing subgraph representation with uni-directional pair-wise representation, we observe that the flow-based GNN architecture is more effective than the GNN used in SumGNN. Even though uni-directional pair-wise representation can achieve better performance compared with all the baselines in S1 setting (Table 1), learning bi-directional representations can help to further improve the prediction ability by balancing the bi-directional communications between drugs.

3 Discussion

Predicting drug-drug interactions (DDI) for emerging drugs is a crucial issue in biomedical computational science as it offers possibilities for treating and alleviating diseases. Despite recent advances in DDI prediction accuracy through the use of deep neural networks [5, 13, 14, 17, 19, 20], these methods require large amount of known DDI information, which is often scarce for emerging drugs. Additionally, some approaches designed for DDI prediction only leverage shallow features, limiting their expressiveness in this task.

One limitation of EmerGNN is that the emerging drug to be predicted should be included in the biomedical network. Building connections between emerging drug and existing drug through molecular formula or property may help address this issue. Although we demonstrate the effectiveness of EmerGNN for DDI prediction in this paper, EmerGNN is a general approach that can be applied to other biomedical applications, such as predicting protein-protein interaction, drug-target interaction and disease-gene interaction. We anticipate that the paths attended by EmerGNN can enhance the accuracy and interpretability of these predictions. We hope that our open-sourced EmerGNN can serve as a strong deep learning tool to advance biomedicine and healthcare, by enabling practitioners to exploit the rich knowledge in existing large biomedical networks for low-data scenarios.

4 Methods

To predict interactions between emerging drugs and existing drugs, it is important to leverage relevant information in the biomedical network. Our framework contains four main components: (i) constructing an augmented network by integrating the DDI network with the biomedical network and adding inverse edges; (ii) extracting all the paths with length no longer than L from u to v to construct a path-based subgraph $\mathcal{G}_{u,v}^L$; (iii) encoding pair-wise subgraph representation $\mathbf{h}_{u,v}^{(L)}$ by a flow-based GNN with attention mechanism such that the information can flow from u over the important entities and edges in $\mathcal{G}_{u,v}^L$ to v ; (iv) predicting the interaction type based on the bi-directional pair-wise subgraph representations. The overall framework is shown in Fig. 1.

Augmented network Given the DDI network $\mathcal{N}_D = \{(u, i, v) : u, v \in \mathcal{V}_D, i \in \mathcal{R}_1\}$ and the biomedical network $\mathcal{N}_B = \{(h, r, t) : h, t \in \mathcal{V}_B, r \in \mathcal{R}_B\}$ (\mathcal{N}_D is specified as $\mathcal{N}_{D\text{-train}}/\mathcal{N}_{D\text{-valid}}/\mathcal{N}_{D\text{-test}}$ in the training/validation/testing stages, respectively, so does \mathcal{N}_B), we integrate the two networks into

$$\mathcal{N}' = \mathcal{N}_D \cup \mathcal{N}_B = \{(e, r, e') : e, e' \in \mathcal{V}', r \in \mathcal{R}'\},$$

with $\mathcal{V}' = \mathcal{V}_D \cup \mathcal{V}_B$ and $\mathcal{R}' = \mathcal{R}_1 \cup \mathcal{R}_B$. The integrated network \mathcal{N}' connects the existing and emerging drugs by concepts in the biomedical network. Since the relation types are directed, we follow the common practices in knowledge graph learning [6, 28] to add inverse types. Specifically, we add r_{inv} for each $r \in \mathcal{R}'$ and create a set of inverse types $\mathcal{R}'_{\text{inv}}$, which subsequently leads to an inverse network

$$\mathcal{N}'_{\text{inv}} = \{(e', r_{\text{inv}}, e) : (e, r, e') \in \mathcal{N}'\}.$$

Note that the inverse relations will not influence the information in the original biomedical network since we can transform any inverse edge (e', r_{inv}, e) back to the original edge (e, r, e') . Semantically, the inverse relations can be regarded as a kind of active voice vs. passive voice in linguistics, for instance *includes_inv* can be regarded as *being included* and *causes_inv* can be regarded as *being caused*. By adding the inverse edges, the paths can be smoothly organized in single directions. For example, a path $a \xrightarrow{r^1} b \xleftarrow{r^2} c$ can be transformed to $a \xrightarrow{r^1} b \xrightarrow{r^2\text{-inv}} c$, which is more computational friendly.

After the above two steps, we obtain the augmented network

$$\mathcal{N} = \mathcal{N}' \cup \mathcal{N}'_{\text{inv}} = \{(e, r, e') : e, e' \in \mathcal{V}, r \in \mathcal{R}\},$$

with entity set $\mathcal{V} = \mathcal{V}' = \mathcal{V}_D \cup \mathcal{V}_B$ and relation set $\mathcal{R} = \mathcal{R}' \cup \mathcal{R}'_{\text{inv}}$.

Path-based subgraph formulation Inspired by the path-based methods in knowledge graph learning [29, 30], we are motivated to extract the paths connecting existing and emerging drugs, and predict the interaction type based on the paths.

Given a drug pair (u, v) to be predicted, we extract the set $\mathcal{P}_{u,v}^L$ of all the paths with length up to L . Each path in $\mathcal{P}_{u,v}^L$ has the form

$$e_0 \xrightarrow{r_1} e_1 \xrightarrow{r_2} \dots \xrightarrow{r_L} e_L,$$

with $e_0 = u$, $e_L = v$ and $(e_{i-1}, r_i, e_i) \in \mathcal{N}$, $i = 1, \dots, L$. The intermediate entities $e_1, \dots, e_{L-1} \in \mathcal{V}$ can be drugs, genes, diseases, side-effects, symptoms, pharmacologic class, etc., and $r_1, \dots, r_L \in \mathcal{R}$ are the interactions or relations between the biomedical entities. In order preserve the local structures, we merge the paths in $\mathcal{P}_{u,v}^L$ to a subgraph $\mathcal{G}_{u,v}^L$ such that the same entities are merged to a single node. The detailed steps of path extraction and subgraph generation are provided in Supplementary Section 1.

Different from the subgraph structures used for link prediction on general graphs [6, 31, 32], the edges in $\mathcal{G}_{u,v}^L$ are pointed away from u and towards v . Our objective is to learn a GNN $g(\cdot)$ with parameters θ that predicts DDI between u and v based on the path-based subgraph $\mathcal{G}_{u,v}^L$, that is

$$\text{DDI}(u, v) = g(\mathcal{G}_{u,v}^L; \theta). \quad (1)$$

The link prediction problem on the DDI network is then transformed as a whole graph learning problem.

Flow-based GNN architecture Given $\mathcal{G}_{u,v}^L$, we would like to integrate essential information in it to predict the target interaction type. Note that the edges in $\mathcal{G}_{u,v}^L$ are from the paths $\mathcal{P}_{u,v}^L$ connecting from u to v . We aim to design a special GNN architecture that the information can flow from drug u to v , via integrating entities and relations in $\mathcal{G}_{u,v}^L$.

Denote $\mathcal{V}_{u,v}^\ell$, $\ell = 0, \dots, L$, as the set of entities that can be visited in the ℓ -th flow step from u (like the four ellipses in $g(\mathcal{G}_{u,v}^L; \theta)$ in Fig. 1). In particular, we have $\mathcal{V}_{u,v}^0 = \{u\}$ as the starting point and $\mathcal{V}_{u,v}^L = \{v\}$ as the ending point. In the ℓ -th iteration, the visible entities in $\mathcal{V}_{u,v}^\ell$ contains entities that are ℓ -steps away from drug u and are $(L - \ell)$ -steps away from drug v in the augmented network \mathcal{N} . We use the fingerprint features [9] of drug u as the input representation of u , namely $\mathbf{h}_{u,u}^{(0)} = \mathbf{f}_u$. Then, we conduct message flow for L steps with the function

$$\mathbf{h}_{u,e}^{(\ell)} = \delta\left(\mathbf{W}^{(\ell)} \sum_{e' \in \mathcal{V}_{u,v}^{\ell-1}} (\mathbf{h}_{u,e'}^{(\ell-1)} + \phi(\mathbf{h}_{u,e'}^{(\ell-1)}, \mathbf{h}_r^{(\ell)}))\right), \quad (2)$$

for entities $e \in \mathcal{V}_{u,v}^\ell$, where $\mathbf{W}^{(\ell)} \in \mathbb{R}^{d \times d}$ is a learnable weighting matrix for step ℓ ; $\mathbf{h}_{u,e'}^{(\ell-1)}$ is the pair-wise representation of entity $e' \in \mathcal{V}_{u,v}^{\ell-1}$; r is the relation type between e' and e ; $\mathbf{h}_r^{(\ell)} \in \mathbb{R}^d$ is the learnable representation with dimension d of r in the ℓ -th step; and $\phi(\cdot, \cdot) : (\mathbb{R}^d, \mathbb{R}^d) \rightarrow \mathbb{R}^d$ is the function combining the two vectors; and $\delta(\cdot)$ is the activation function ReLU [33].

Since the biomedical network is not specially designed for the DDI prediction task, we need to control the importance of different edges in $\mathcal{G}_{u,v}^L$. We use a

drug-dependent attention weight for function $\phi(\cdot, \cdot)$. Specifically, we design the message function for each edge (e', r, e) during the l -th propagation step as

$$\phi(\mathbf{h}_{u,e'}^{(\ell-1)}, \mathbf{h}_r^{(\ell)}) = \alpha_r^{(\ell)} \cdot \left(\mathbf{h}_{u,e'}^{(\ell-1)} \odot \mathbf{h}_r^{(\ell)} \right), \quad (3)$$

where \odot is an element-wise dot product of vectors and $\alpha_r^{(\ell)}$ is the attention weight controlling the importance of messages. We design the attention weight depending on the edges' relation type as

$$\alpha_r^{(\ell)} = \sigma \left((\mathbf{w}_r^{(\ell)})^\top [\mathbf{f}_u; \mathbf{f}_v] \right),$$

where the relation weight $\mathbf{w}_r^{(\ell)} \in \mathbb{R}^{2d}$ is multiplied with the fingerprints $[\mathbf{f}_u; \mathbf{f}_v] \in \mathbb{R}^{2d}$ of drugs to be predicted and $\sigma(\cdot)$ is a sigmoid function returning a value in $(0, 1)$.

After iterating for L steps, we can obtain the representation $\mathbf{h}_{u,v}^{(L)}$ that encodes the important paths up to length L between drugs u and v .

Objective and training In practice, the interaction types can be symmetric, for example #Drug1 and #Drug2 may have the side effect of headache if used together, or asymmetric, for example #Drug1 may decrease the analgesic activities of #Drug2. Besides, the emerging drug can appear in either the source (drug u) or target (drug v). We extract the reverse subgraph $\mathcal{G}_{v,u}^L$ and encode it with the same parameters in Equation (2) to obtain the reverse pair-wise representation $\mathbf{h}_{v,u}^{(L)}$. Then the bi-directional representations are concatenated to predict the interaction type with

$$\mathbf{l}(u, v) = \mathbf{W}_{\text{rel}} \left[\mathbf{h}_{u,v}^{(L)}; \mathbf{h}_{v,u}^{(L)} \right]. \quad (4)$$

Here, the transformation matrix $\mathbf{W}_{\text{rel}} \in \mathbb{R}^{|\mathcal{R}_I| \times 2d}$ is used to map the pair-wise representations into prediction logits $\mathbf{l}(u, v)$ of the $|\mathcal{R}_I|$ interaction types. The i -th logit $l_i(u, v)$ indicates the plausibility of interaction type i being predicted. The full algorithm and implementation details of Equation (4) are provided in Supplementary Section 1.

Since we have two kinds of tasks that are multi-class (on the DrugBank dataset) and multi-label (on the TWOSIDES dataset) interaction predictions, the training objectives are different.

For DrugBank, there exists at most one interaction type between two drugs. Given two drugs u and v , once we obtain the prediction logits $\mathbf{l}(u, v)$ of different interaction types, we use a softmax function to compute the probability of each interaction type, namely

$$I_i(u, v) = \frac{\exp(l_i(u, v))}{\sum_{j \in \mathcal{R}_I} \exp(l_j(u, v))}.$$

Denote $\mathbf{y}(u, v) \in \mathbb{R}^{|\mathcal{R}_i|}$ as the ground-truth indicator of target interaction type, where $y_i(u, v) = 1$ if $(u, i, v) \in \mathcal{N}_D$, otherwise zero. We minimize the following cross-entropy loss to train the model parameters

$$\mathcal{L}_{DB} = - \sum_{(u, i, v) \in \mathcal{N}_{D\text{-train}}} y_i(u, v) \log I_i(u, v). \quad (5)$$

For TWOSIDES, there may be multiple interactions between two drugs. The objective is to predict whether there is an interaction p between two drugs. Given two drugs u, v and the prediction logits $\mathbf{l}(u, v)$, we use the sigmoid function

$$I_i(u, v) = \frac{1}{1 + \exp(-l_i(u, v))},$$

to compute the probability of interaction type i . Different with the multi-class task in DrugBank, we use the binary cross entropy loss

$$\mathcal{L}_{TS} = - \sum_{(u, i, v) \in \mathcal{N}_{D\text{-train}}} \left(\log(I_i(u, v)) + \sum_{(u', v') \in \mathcal{N}_i} \log(1 - I_i(u', v')) \right), \quad (6)$$

where \mathcal{N}_i is the set of drug pairs that do not have the interaction type i .

We use stochastic gradient optimizer Adam [34] to optimize the model parameters

$$\boldsymbol{\theta} = \left\{ \mathbf{W}_{\text{rel}}, \{ \mathbf{W}^{(\ell)}, \mathbf{h}_r^{(\ell)}, \mathbf{w}_r^{(\ell)} \}_{\ell=1, \dots, L, r \in \mathcal{R}} \right\},$$

by minimizing loss function in Equation (5) for the DrugBank dataset or Equation (6) for the TWOSIDES dataset.

Drug-drug interaction network. Following [6, 13], we use two benchmark datasets, DrugBank [22] and TWOSIDES [23], as the interaction network \mathcal{N}_D (Supplementary Table 1). When predicting DDIs for emerging drugs, namely the S1 and S2 settings, we randomly split \mathcal{V}_D into three disjoint sets with $\mathcal{V}_D = \mathcal{V}_{D\text{-train}} \cup \mathcal{V}_{D\text{-valid}} \cup \mathcal{V}_{D\text{-test}}$ and $\mathcal{V}_{D\text{-train}} \cap \mathcal{V}_{D\text{-valid}} \cap \mathcal{V}_{D\text{-test}} = \emptyset$, where $\mathcal{V}_{D\text{-train}}$ is the set of existing drugs used for training, $\mathcal{V}_{D\text{-valid}}$ is the set of emerging drugs for validation, and $\mathcal{V}_{D\text{-test}}$ is the set of emerging drugs for testing. The interaction network for training is defined as $\mathcal{N}_{D\text{-train}} = \{(u, i, v) \in \mathcal{N}_D : u, v \in \mathcal{V}_{D\text{-train}}\}$.

In the S1 setting, we set

- $\mathcal{N}_{D\text{-valid}} = \{(u, i, v) \in \mathcal{N}_D : u \in \mathcal{V}_{D\text{-train}}, v \in \mathcal{V}_{D\text{-valid}}\} \cup \{(u, i, v) \in \mathcal{N}_D : u \in \mathcal{V}_{D\text{-valid}}, v \in \mathcal{V}_{D\text{-train}}\}$ as validation samples;
- $\mathcal{N}_{D\text{-test}} = \{(u, i, v) \in \mathcal{N}_D : u \in (\mathcal{V}_{D\text{-train}} \cup \mathcal{V}_{D\text{-valid}}), v \in \mathcal{V}_{D\text{-test}}\} \cup \{(u, i, v) \in \mathcal{N}_D : u \in \mathcal{D}_{D\text{-test}}, v \in (\mathcal{V}_{D\text{-train}} \cup \mathcal{V}_{D\text{-valid}})\}$ as testing samples.

In the S2 setting, we set

- $\mathcal{N}_{D\text{-valid}} = \{(u, i, v) \in \mathcal{N}_D : u, v \in \mathcal{V}_{D\text{-valid}}\}$ as validation samples; and

- $\mathcal{N}_{\text{D-test}} = \{(u, i, v) \in \mathcal{N}_{\text{D}} : u, v \in \mathcal{V}_{\text{D-test}}\}$ as testing samples.

We follow [6] to randomly sample one negative sample for each $(u, i, v) \in \mathcal{N}_{\text{D-valid}} \cup \mathcal{N}_{\text{D-test}}$ to form the negative set \mathcal{N}_i for TWOSIDES dataset in the evaluation phase. Specifically, if u is an emerging drug, we randomly sample an existing drug $v' \in \mathcal{V}_{\text{D-train}}$ and make sure that the new interaction does not exist, namely $(u, i, v') \notin \mathcal{N}_{\text{D}}$; if v is an emerging drug, we randomly sample an existing drug $u' \in \mathcal{V}_{\text{D-train}}$ and make sure that the new interaction does not exist, namely $(u', i, v) \notin \mathcal{N}_{\text{D}}$.

Biomedical network. In this work, same as the DDI network, we use different variants of the biomedical network \mathcal{N}_{B} for training, validation and testing. The well-built biomedical network HetioNet [18] is used here. Denote $\mathcal{V}_{\text{B}}, \mathcal{R}_{\text{B}}, \mathcal{N}_{\text{B}}$ as the set of entities, relations and edges, respectively, in the full biomedical network. When predicting interactions between existing drugs in the S0 setting, all the edges in \mathcal{N}_{B} are used for training, validation and testing. When predicting interactions between emerging drugs and existing drugs (S1 and S2 setting), we use different parts of the biomedical networks.

In order to guarantee that the emerging drugs are connected with some existing drugs through the biomedical entities, we constrain the split of drugs to satisfy the conditions $\mathcal{V}_{\text{D-valid}} \subset \mathcal{V}_{\text{B}}$ and $\mathcal{V}_{\text{D-test}} \subset \mathcal{V}_{\text{B}}$. Meanwhile, we also guarantee that the emerging drugs will not be seen in the biomedical network during training. To achieve this goal, the edges for training are in the set $\mathcal{N}_{\text{B-train}} = \{(h, r, t) \in \mathcal{N}_{\text{B}} : h, t \notin (\mathcal{V}_{\text{D-valid}} \cup \mathcal{V}_{\text{D-test}})\}$; the edges for validation are in the set $\mathcal{N}_{\text{B-valid}} = \{(h, r, t) \in \mathcal{N}_{\text{B}} : h, t \notin \mathcal{V}_{\text{D-test}}\}$; and the testing network is the original network, namely $\mathcal{N}_{\text{B-test}} = \mathcal{N}_{\text{B}}$.

In addition, we plot the size distribution (measured by the number of edges in $\mathcal{G}_{u,v}^L$) as histograms (Supplementary Figure 1). We observe that both datasets follow long-tail distributions. Many subgraphs have tens of thousands of edges on DrugBank, while hundreds of thousands of edges on TWOSIDES since the DDI network is denser. Comparing with the augmented networks, whose sizes are 3,657,114 for DrugBank and 3,567,059 for TWOSIDES, the sizes of subgraphs are quite small.

Evaluation metrics. As pointed by [6], there is at most one interaction between a pair of drugs in the DrugBank dataset [22]. Hence, we evaluate the performance in a multi-class setting, which estimates whether the model can correctly predict the interaction type for a pair of drugs. We consider the following metrics:

- $\text{F1}(\text{macro}) = \frac{1}{\|\mathcal{I}_{\text{D}}\|} \sum_{i \in \mathcal{I}_{\text{D}}} \frac{2P_i R_i}{P_i + R_i}$, where P_i and R_i are the precision and recall for the interaction type i , respectively. The macro F1 aggregates the fractions over different interaction types.
- Accuracy: the percentage of correctly predicted interaction type compared with the ground-truth interaction type.

- Cohen’s Kappa [24]: $\kappa = \frac{A_p - A_e}{1 - A_e}$, where A_p is the observed agreement (accuracy) and A_e is the probability of randomly seeing each class.

In the TWOSIDES dataset [23], there may be multiple interactions between a pair of drugs, such as anaemia, nausea and pain. Hence, we model and evaluate the performance in a multi-label setting, where each type of side effect is modeled as a binary classification problem. Following [13, 23], we sample one negative drug pair for each $(u, i, v) \in \mathcal{N}_{\text{D-test}}$ and evaluate the binary classification performance with the following metrics:

- ROC-AUC: the area under curve of receiver operating characteristics, measured by $\sum_{k=1}^n \text{TP}_k \Delta \text{FP}_k$, where $(\text{TP}_k, \text{FP}_k)$ is the true-positive and false-positive of the k -th operating point.
- PR-AUC: the area under curve of precision-recall, measured by $\sum_{k=1}^n P_k \Delta R_k$, where (P_k, R_k) is the precision and recall of the k -th operating point.
- Accuracy: the average precision of drug pairs for each side effect.

Data availability

Source data for Figures 2-5 is available with this manuscript. The resplit dataset [35] of DrugBank, TWOSIDES and HetioNet for S1 and S2 settings is public available at <https://doi.org/10.5281/zenodo.10016715>.

Code availability

The code for EmerGNN [36] is available at <https://github.com/LARS-research/EmerGNN>.

Acknowledgments

This project was supported by the National Natural Science Foundation of China (No. 92270106) and CCF-Tencent Open Research Fund.

Author Contributions Statement

Y. Zhang contributes to idea development, algorithm implementation, experimental design, result analysis, and paper writing. Q. Yao contributes to idea development, experimental design, result analysis, and paper writing. L. Yue contributes to algorithm implementation and result analysis. Y. Zheng contributes to result analysis and paper writing. All authors read, edited, and approved the paper.

Competing Interests Statement

The authors declare no competing interests.

Tables

Table 1: Performance of EmerGNN compared other DDI prediction methods. Four types of DDI prediction methods are compared: (i) methods that use drug features of target drug pairs (*DF*) [4, 9, 11, 21]; (ii) methods that use graph features in the biomedical network (*GF*) [5]; (iii) methods that learn drug embeddings (*Emb*) [12, 14]; and (iv) methods that model with GNNs (*GNN*) [6, 13, 16, 17, 28].

S1 Setting: DDI prediction between emerging drug and existing drug ¹.

Datasets		DrugBank			TWO SIDES		
Type	Methods	F1-Score	Accuracy	Kappa	PR-AUC	ROC-AUC	Accuracy
DF	MLP [9]	21.1±0.8	46.6±2.1	33.4±2.5	81.5±1.5	81.2±1.9	76.0±2.1
	Similarity [4]	43.0±5.0	51.3±3.5	44.8±3.8	56.2±0.5	55.7±0.6	53.9±0.4
	CSMDDI [11]	45.5±1.8	<u>62.6±2.8</u>	<u>55.0±3.2</u>	73.2±2.6	74.2±2.9	69.9±2.2
	STNN-DDI [21]	39.7±1.8	56.7±2.6	46.5±3.4	68.9±2.0	68.3±2.6	65.3±1.8
GF	HIN-DDI* [5]	37.3±2.9	58.9±1.4	47.6±1.8	<u>81.9±0.6</u>	<u>83.8±0.9</u>	<u>79.3±1.1</u>
Emb	MSTE [12]	7.0±0.7	51.4±1.8	37.4±2.2	64.1±1.1	62.3±1.1	58.7±0.7
	KG-DDI* [14]	26.1±0.9	46.7±1.9	35.2±2.5	79.1±0.9	77.7±1.0	60.2±2.2
GNN	CompGCN* [28]	26.8±2.2	48.7±3.0	37.6±2.8	80.3±3.2	79.4±4.0	71.4±3.1
	Decagon* [13]	24.3±4.5	47.4±4.9	35.8±5.9	79.0±2.0	78.5±2.3	69.7±2.4
	KGNN* [16]	23.1±3.4	51.4±1.9	40.3±2.7	78.5±0.5	79.8±0.6	72.3±0.7
	SumGNN* [6]	35.0±4.3	48.8±8.2	41.1±4.7	80.3±1.1	81.4±1.0	73.0±1.4
	DeepLGF* [17]	39.7±2.3	60.7±2.4	51.0±2.6	81.4±2.1	82.2±2.6	72.8±2.8
	EmerGNN*	62.0±2.0	68.6±3.7	62.4±4.3	90.6±0.7	91.5±1.0	84.6±0.7
p-value		8.9E-7	0.02	0.02	1.6E-6	6.0E-8	3.5E-5

S2 Setting: DDI prediction between two emerging drugs.

Datasets		DrugBank			TWO SIDES		
Type	Methods	F1-Score	Accuracy	Kappa	PR-AUC	ROC-AUC	Accuracy
DF	CSMDDI [11]	<u>19.8±3.1</u>	<u>37.3±4.8</u>	<u>22.0±4.9</u>	55.8±4.9	57.0±6.1	55.1±5.2
GF	HIN-DDI* [5]	8.8±1.0	27.6±2.4	13.8±2.4	<u>64.8±2.3</u>	<u>58.5±1.6</u>	<u>59.8±1.4</u>
Emb	KG-DDI* [14]	1.1±0.1	32.2±3.6	0.0±0.0	53.9±3.9	47.0±5.5	50.0±0.0
GNN	DeepLGF* [17]	4.8±1.9	31.9±3.7	8.2±2.3	59.4±8.7	54.7±5.9	54.0±6.2
	EmerGNN*	25.0±2.8	46.3±3.6	31.9±3.8	81.4±7.4	79.6±7.9	73.0±8.2
p-value		0.02	0.01	0.01	1.4E-3	3.9E-4	7.8E-3

¹All of the methods are run for five times on the five-fold datasets with mean value and standard deviation reported on the testing data. The evaluation metrics are presented in percentage (%) with the larger value indicating better performance. The boldface numbers indicate the best values, while the underlined numbers indicate the second best. p-values are computed under two-sided t-testing of EmerGNN over the second best baselines. Methods leveraging a biomedical network are indicated by star *.

Figures

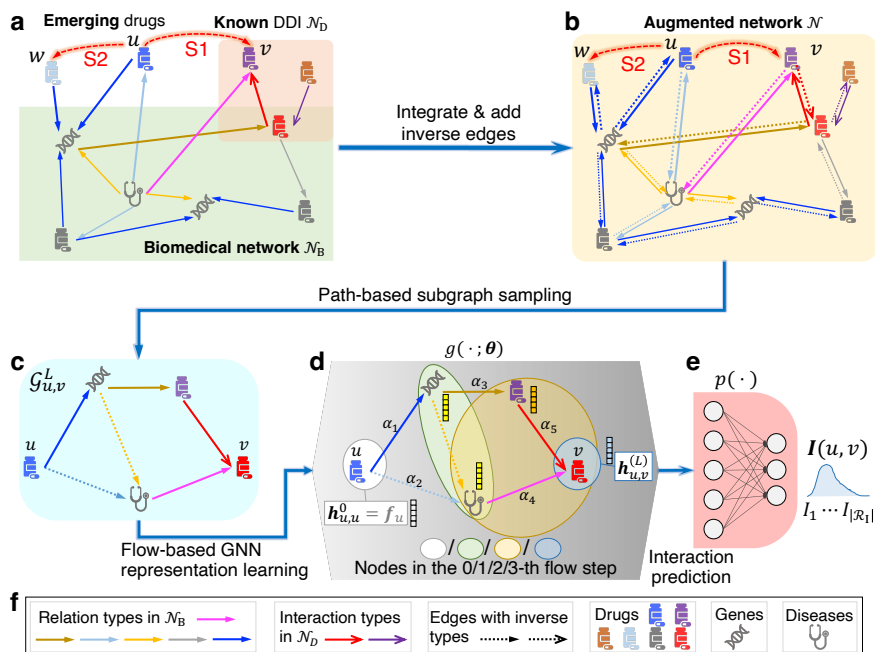


Figure 1: **Overview of EmerGNN.** (a) Problem formulation: Given a DDI network \mathcal{N}_D of existing drugs and a large biomedical network \mathcal{N}_B providing side information for the drugs, the task is to predict the interaction type between an emerging drug (like u in dark blue) and an existing drug (like v in purple) in the S1 setting, or interaction type between two emerging drugs (like u in dark blue and w in light blue) in the S2 setting. (b) Augmented network \mathcal{N} : The DDI network and biomedical network are integrated and edges with inverse types are incorporated to obtain an augmented network \mathcal{N} . The augmentation brings better communication among drugs and entities in both interaction and biomedical networks. (c) Path-based subgraph: Given a drug pair (u, v) to be predicted, all the paths from u to v with length no larger than L are extracted to construct a path-based subgraph $\mathcal{G}_{u,v}^L$. (d) Flow-based GNN $g(\cdot; \theta)$ with parameters θ : the network flows the initial drug features $\mathbf{h}_{u,u}^0 = \mathbf{f}_u$ over essential information in $\mathcal{G}_{u,v}^L$ for L steps. It uses different attention weights α 's to weight the importance of different edges. After L steps, a pair-wise representation $\mathbf{h}_{u,v}^L$ between u and v is obtained as the subgraph representation of $\mathcal{G}_{u,v}^L$. (e) Interaction predictor $p(\cdot)$: a simple linear classifier $p(\mathbf{h}_{u,v}^L)$ outputs a distribution $\mathbf{I}(u, v)$, where each dimension indicates an interaction type $i \in \mathcal{R}_I$ between u and v . (f) Legends: The different relation and interaction types are indicated by arrows with different colors. Edges with inverse types are indicated by dashed arrows with corresponding color. The icons represent biomedical concepts including drugs, genes and diseases.

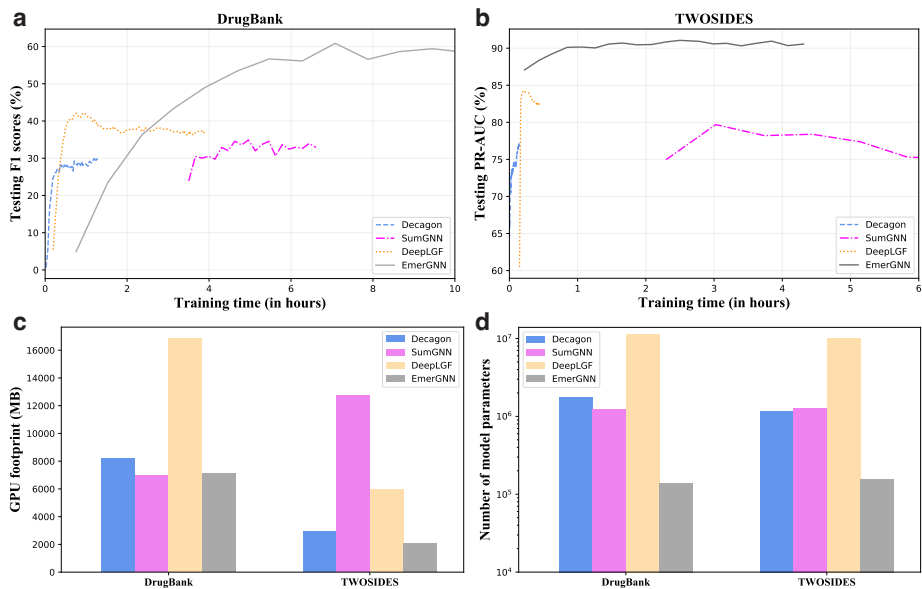


Figure 2: Complexity analysis of different GNN-based methods in the S1 setting. **(a)** Comparison of training curves on DrugBank dataset. **(b)** Comparison of training curves on TWOSIDES dataset. **(c)** Comparison of GPU memory footprint usage on the two datasets in MB. **(d)** Comparison of number of trainable model parameters on the two datasets.

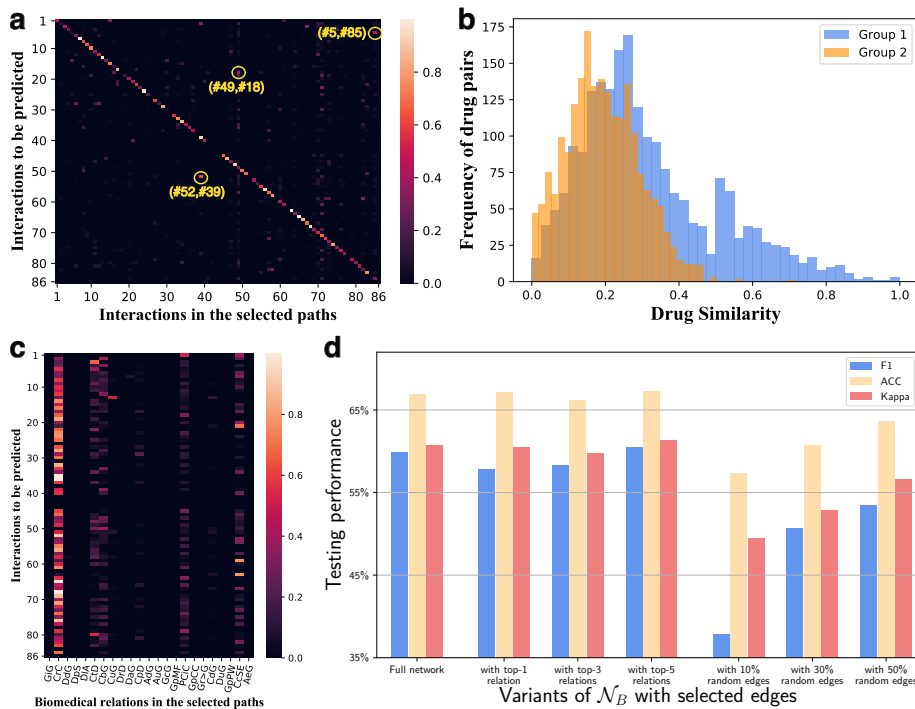


Figure 3: Analysis of relation types on the selected paths on the DrugBank dataset. In detail, we first extract top five paths from u to v and from v to u , respectively, for each triplet (u, i_{pred}, v) in testing based on the average attention weights of edges in each path with a beam search algorithm (Algorithm 2 in Supplementary Section 1). Next, we count how many times an interaction type $i \in \mathcal{R}_I$ and a relation type $r \in \mathcal{R}_B$ appears on the selected edges given i_{pred} (Supplementary Figure 3). **(a)** Heatmap of correlation between interaction i_{pred} to be predicted and interaction types i in the selected paths. Yellow circles indicate the three highlighted interaction pairs outside the diagonal (Supplementary Table 5). **(b)** The histogram distribution of fingerprint similarities in *Group 1* (a drug u with another drug u_1 , which connected to v with interaction type i_{pred}) and *Group 2* (a drug u with a random drug u_2). **(c)** Heatmap of correlation between interaction i_{pred} to be predicted and biomedical relations r in the selected paths. **(d)** Performance of modified biomedical networks with selected relations. Leftmost is the performance of EmerGNN with full biomedical network. The middle three parts are EmerGNN with top-1 (CrC, with 0.4% edges), top-3 (CrC, CbG, CsSE, with 9.3% edges), top-5 (CrC, CtD, CvG, PCiC, CsSE, with 9.4% edges) attended relations in the biomedical network. The right three parts are EmerGNN with randomly sampled 10%, 30%, 50% edges from the biomedical network.

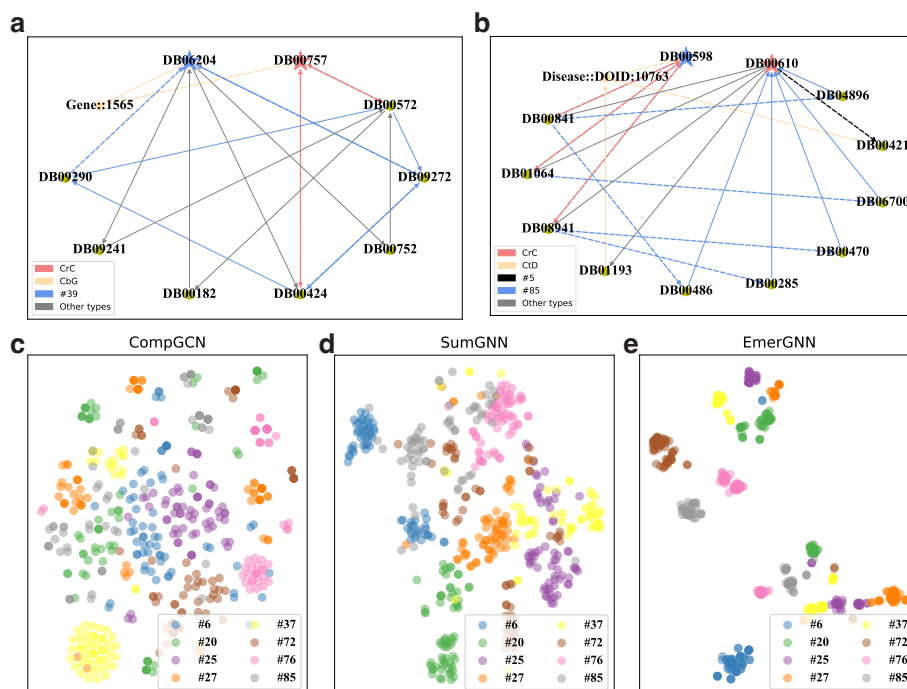


Figure 4: Visualization of drug pairs. **(a-b)** Two cases of subgraphs containing top ten paths according to the average of edges’ attention weights on each path (explanations in Supplementary Table 6). The drug pairs to be predicted are highlighted as stars; dashed lines mean reverse types; CrC, CbG, CtD are biomedical relations; #39, #5, #85 are interaction types; “other types” in gray edges mean the interaction types aside from the given ones. In the first case, DB06204 (Tapentadol) in blue star is an existing drug, and DB00757 (Dolasetron) in red star is an emerging drug. The target interaction type is “#Drug1 may decrease the analgesic activities of #Drug2” (#52). In the second case, DB00598 (Labetalol) in blue star is an emerging drug, and DB00610 (Metaraminol) in red star is an existing drug. The target interaction type is “#Drug1 may decrease the vasoconstricting activities of #Drug2” (#5). **(c-e)** t-SNE visualization [37] of the representations learned for drug pairs. As CompGCN embeds each entity separately, we concatenate embeddings of the two drugs’ representations for a given drug pair. SumGNN encodes the enclosing subgraphs of (u, v) for interaction prediction, thus we take the representation of enclosing subgraph as the drug pair representation. The drug pair representation of EmerGNN is directly given by $\mathbf{h}_{u,v}^{(L)}$. Since there are too many interaction types and drug pairs in $\mathcal{N}_{D\text{-test}}$, eight interaction types and sixty-four drug pairs are randomly sampled for each interaction type. The legends in these figures specify the IDs of the interaction type to be predicted; each dot denotes a DDI sample (u, i, v) ; the different colors in dots indicate the interaction type i that the drug pairs (u, v) have.

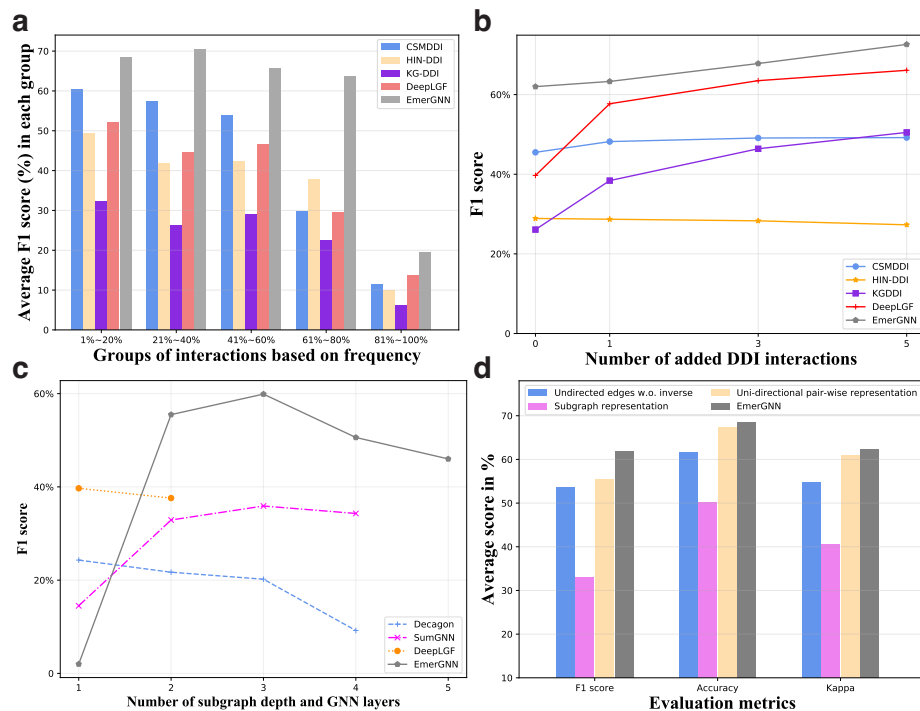


Figure 5: Ablation studies on the DrugBank dataset. **(a)** Performance comparison of interaction groups based on interaction frequency. The five groups are formed by grouping the interaction types based on their frequency in the dataset, and the average macro F1 performance is shown in each group. **(b)** Performance comparison of adding interaction edges for emerging drugs into the training set $\mathcal{N}_{D-\text{train}}$. Specifically, 1/3/5 interaction edges in the testing set $\mathcal{N}_{D-\text{test}}$ are randomly sampled for each emerging drug in $\mathcal{V}_{D-\text{test}}$, and moved to the training set $\mathcal{N}_{D-\text{train}}$. **(c)** Performance comparison of GNN-based methods by varying the depth L . Specifically, L means the number of GNN layers in Decagon and DeepLGF, the depth of enclosing subgraph in SumGNN, and the depth of path-based subgraph in EmerGNN. **(d)** Performance comparison of different technique designing in EmerGNN (Supplementary Table 7).

References

- [1] Xian Su, Haixue Wang, Nan Zhao, Tao Wang, and Yimin Cui. Trends in innovative drug development in China. Nature Reviews. Drug Discovery, 2022.
- [2] Heidi Ledford. Hundreds of COVID trials could provide a deluge of new drugs. Nature, pages 25–27, 2022.
- [3] Bethany Percha and Russ B Altman. Informatics confronts drug-drug interactions. Trends in Pharmacological Sciences, 34(3):178–184, 2013.
- [4] Santiago Vilar, Eugenio Uriarte, Lourdes Santana, Tal Lorberbaum, George Hripcsak, Carol Friedman, and Nicholas P Tatonetti. Similarity-based modeling in large-scale prediction of drug-drug interactions. Nature Protocols, 9(9):2147–2163, 2014.
- [5] Farhan Tanvir, Muhammad Ifta Khairul Islam, and Esra Akbas. Predicting drug-drug interactions using meta-path based similarities. In IEEE Conference on Computational Intelligence in Bioinformatics and Computational Biology, pages 1–8. IEEE, 2021.
- [6] Yue Yu, Kexin Huang, Chao Zhang, Lucas M Glass, Jimeng Sun, and Cao Xiao. SumGNN: multi-typed drug interaction prediction via efficient knowledge graph summarization. Bioinformatics, 37(18):2988–2995, 2021.
- [7] Louis Letinier, Sebastien Cossin, Yohann Mansiaux, Mickael Arnaud, Francesco Salvo, Julien Bezin, Frantz Thiessard, and Antoine Pariente. Risk of drug-drug interactions in out-hospital drug dispensings in France: Results from the drug-drug interaction prevalence study. Frontiers in Pharmacology, 10:265, 2019.
- [8] Huaqiao Jiang, Yanhua Lin, Weifang Ren, Zhonghong Fang, Yujuan Liu, Xiaofang Tan, Xiaoqun Lv, and Ning Zhang. Adverse drug reactions and correlations with drug-drug interactions: A retrospective study of reports from 2011 to 2020. Frontiers in Pharmacology, 13, 2022.
- [9] David Rogers and Mathew Hahn. Extended-connectivity fingerprints. Journal of Chemical Information and Modeling, 50(5):742–754, 2010.
- [10] Pieter Dewulf, Michiel Stock, and Bernard De Baets. Cold-start problems in data-driven prediction of drug-drug interaction effects. Pharmaceuticals, 14(5):429, 2021.
- [11] Zun Liu, Xing-Nan Wang, Hui Yu, Jian-Yu Shi, and Wen-Min Dong. Predict multi-type drug-drug interactions in cold start scenario. BMC Bioinformatics, 23(1):75, 2022.

- [12] Junfeng Yao, Wen Sun, Zhongquan Jian, Qingqiang Wu, and Xiaoli Wang. Effective knowledge graph embeddings based on multidirectional semantics relations for polypharmacy side effects prediction. Bioinformatics, 38(8): 2315–2322, 2022.
- [13] Marinka Zitnik, Monica Agrawal, and Jure Leskovec. Modeling polypharmacy side effects with graph convolutional networks. Bioinformatics, 34(13):i457–i466, 2018.
- [14] Md Rezaul Karim, Michael Cochez, Joao Bosco Jares, Mamta Uddin, Oya Beyan, and Stefan Decker. Drug-drug interaction prediction based on knowledge graph embeddings and convolutional-LSTM network. In Proceedings of the 10th ACM International Conference on Bioinformatics, Computational Biology and Health Informatics, pages 113–123, 2019.
- [15] Kexin Huang, Cao Xiao, Lucas M Glass, Marinka Zitnik, and Jimeng Sun. SkipGNN: predicting molecular interactions with skip-graph networks. Scientific Reports, 10(1):1–16, 2020.
- [16] Xuan Lin, Zhe Quan, Zhi-Jie Wang, Tengfei Ma, and Xiangxiang Zeng. KGNN: Knowledge graph neural network for drug-drug interaction prediction. In Proceedings of the Twenty-Ninth International Conference on International Joint Conferences on Artificial Intelligence, volume 380, pages 2739–2745, 2020.
- [17] Zhong-Hao Ren, Zhu-Hong You, Chang-Qing Yu, Li-Ping Li, Yong-Jian Guan, Lu-Xiang Guo, and Jie Pan. A biomedical knowledge graph-based method for drug-drug interactions prediction through combining local and global features with deep neural networks. Briefings in Bioinformatics, 23(5):bbac363, 2022.
- [18] Daniel Scott Himmelstein, Antoine Lizee, Christine Hessler, Leo Brueggeman, Sabrina L Chen, Dexter Hadley, Ari Green, Pouya Khankhanian, and Sergio E Baranzini. Systematic integration of biomedical knowledge prioritizes drugs for repurposing. Elife, 6:e26726, 2017.
- [19] Thomas N Kipf and Max Welling. Semi-supervised classification with graph convolutional networks. In International Conference on Learning Representations, 2016.
- [20] Justin Gilmer, Samuel S Schoenholz, Patrick F Riley, Oriol Vinyals, and George E Dahl. Neural message passing for quantum chemistry. In International Conference on Machine Learning, pages 1263–1272. PMLR, 2017.
- [21] Hui Yu, ShiYu Zhao, and JianYu Shi. STNN-DDI: a substructure-aware tensor neural network to predict drug-drug interactions. Briefings in Bioinformatics, 23(4):bbac209, 2022.

- [22] David S Wishart, Yannick D Feunang, An C Guo, Elvis J Lo, Ana Marcu, Jason R Grant, Tanvir Sajed, Daniel Johnson, Carin Li, Zinat Sayeeda, et al. DrugBank 5.0: a major update to the DrugBank database for 2018. Nucleic Acids Research, 46(D1):D1074–D1082, 2018.
- [23] Nicholas P Tatonetti, Patrick P Ye, Roxana Daneshjou, and Russ B Altman. Data-driven prediction of drug effects and interactions. Science translational medicine, 4(125):125ra31–125ra31, 2012.
- [24] Jacob Cohen. A coefficient of agreement for nominal scales. Educational and Psychological Measurement, 20(1):37–46, 1960.
- [25] Dean G Brown, Heike J Wobst, Abhijeet Kapoor, Leslie A Kenna, and Noel Southall. Clinical development times for innovative drugs. Nature reviews. Drug discovery, 21(11):793–794, 2021.
- [26] Maywin Liu and Eric Wittbrodt. Low-dose oral naloxone reverses opioid-induced constipation and analgesia. Journal of Pain and Symptom Management, 23(1):48–53, 2002.
- [27] Ronald W Estabrook. A passion for P450s (remembrances of the early history of research on cytochrome P450). Drug Metabolism and Disposition, 31(12):1461–1473, 2003.
- [28] Shikhar Vashishth, Soumya Sanyal, Vikram Nitin, and Partha Talukdar. Composition-based multi-relational graph convolutional networks. In International Conference on Learning Representations, 2019.
- [29] Ni Lao, Tom Mitchell, and William Cohen. Random walk inference and learning in a large scale knowledge base. In Proceedings of the 2011 Conference on Empirical Methods in Natural Language Processing, pages 529–539, 2011.
- [30] Wenhan Xiong, Thien Hoang, and William Yang Wang. DeepPath: A reinforcement learning method for knowledge graph reasoning. In Proceedings of the 2017 Conference on Empirical Methods in Natural Language Processing, pages 564–573, 2017.
- [31] Muhan Zhang and Yixin Chen. Link prediction based on graph neural networks. In Proceedings of the 32nd International Conference on Neural Information Processing Systems, pages 5171–5181, 2018.
- [32] Komal Teru, Etienne Denis, and Will Hamilton. Inductive relation prediction by subgraph reasoning. In International Conference on Machine Learning, pages 9448–9457. PMLR, 2020.
- [33] Vinod Nair and Geoffrey E Hinton. Rectified linear units improve restricted Boltzmann machines. In Proceedings of the 27th International Conference on Machine Learning, pages 807–814, 2010.

- [34] D. P Kingma and J. Ba. Adam: A method for stochastic optimization. Technical report, arXiv:1412.6980, 2014.
- [35] Yongqi Zhang, Ling Yue, and Quanming Yao. EmerGNN_DDI_data, October 2023.
- [36] Yongqi Zhang, Ling Yue, and Quanming Yao. EmerGNN, 10 2023. URL <https://github.com/LARS-research/EmerGNN>.
- [37] Laurens Van der Maaten and Geoffrey Hinton. Visualizing data using t-SNE. Journal of Machine Learning Research, 9(11), 2008.
- [38] James Bergstra, Brent Komer, Chris Eliasmith, Dan Yamins, and David D Cox. Hyperopt: A Python library for model selection and hyperparameter optimization. Computational Science & Discovery, 8(1):014008, 2015.
- [39] Raheel Chaudhry, Julia H Miao, and Afzal Rehman. Physiology, cardiovascular. In StatPearls [Internet]. StatPearls Publishing, 2022.
- [40] Keyulu Xu, Weihua Hu, Jure Leskovec, and Stefanie Jegelka. How powerful are graph neural networks? In International Conference on Learning Representations, 2018.

Supplementary Section 1 Algorithms

Algorithm for EmerGNN. In this part, we show the full algorithm and some implementation details of EmerGNN. Given the augmented network \mathcal{N} and the drug pairs (u, v) , it will be time consuming to explicitly extract all the paths connecting u and v with length $\leq L$. In practice, we implicitly encode the pair-wise representations with Algorithm 1.

Algorithm 1 EmerGNN: pair-wise representation learning with flow-based GNN.

Require: $(u, v), L, \delta, \sigma, \{\mathbf{W}^{(\ell)}, \mathbf{w}^{(\ell)}\}_{\ell=1\dots L}$.

$\{(u, v)$: drug pair; L : the depth of path-based subgraph; δ : activation function; σ : sigmoid function; $\{\mathbf{W}^{(\ell)}, \mathbf{w}^{(\ell)}\}_{\ell=1\dots L}$: learnable parameters.}

- 1: initialize the $u \rightarrow v$ pair-wise representation as $\mathbf{h}_{u,e}^0 = \mathbf{f}_u$ if $e = u$, otherwise $\mathbf{h}_{u,e}^0 = \mathbf{0}$;
 - 2: initialize the $v \rightarrow u$ pair-wise representation as $\mathbf{h}_{v,e}^0 = \mathbf{f}_v$ if $e = v$, otherwise $\mathbf{h}_{v,e}^0 = \mathbf{0}$;
 - 3: **for** $\ell \leftarrow 1$ to L **do**
 - 4: **for** $e \in \mathcal{V}_D$ **do** {This loop can work with matrix operations in parallel.}
 - 5: message for $u \rightarrow v$:

$$\mathbf{h}_{u,e}^{(\ell)} = \delta \left(\mathbf{W}^{(\ell)} \sum_{(e',r,e) \in \mathcal{N}_D} \sigma \left((\mathbf{w}_r^{(\ell)})^\top [\mathbf{f}_u; \mathbf{f}_v] \right) \cdot \left(\mathbf{h}_{u,e'}^{(\ell-1)} \odot \mathbf{h}_r^{(\ell)} \right) \right);$$
 - 6: message for $v \rightarrow u$:

$$\mathbf{h}_{v,e}^{(\ell)} = \delta \left(\mathbf{W}^{(\ell)} \sum_{(e',r,e) \in \mathcal{N}_D} \sigma \left((\mathbf{w}_r^{(\ell)})^\top [\mathbf{f}_u; \mathbf{f}_v] \right) \cdot \left(\mathbf{h}_{v,e'}^{(\ell-1)} \odot \mathbf{h}_r^{(\ell)} \right) \right);$$
 - 7: **end for**
 - 8: **end for**
 - 9: **Return** $\mathbf{W}_{\text{rel}}[\mathbf{h}_{u,v}^{(L)}, \mathbf{h}_{v,u}^{(L)}]$.
-

Take the direction $u \rightarrow v$ as an example. We initialize the representation $\mathbf{h}_{u,e}^0 = \mathbf{f}_u$ if $e = u$, otherwise $\mathbf{h}_{u,e}^0 = \mathbf{0}$ and the messages are computed based on a dot product operator $\mathbf{h}_{u,e'}^{(\ell-1)} \odot \mathbf{h}_r^{(\ell)}$, then the representations of all entities with length longer than ℓ away from u will be $\mathbf{0}$ in the ℓ -th step. In the end, only the entities with length $\leq L$ will have valid representations. In addition, since we return $\mathbf{h}_{u,v}^{(L)}$ for specific entity v , only the entities with length less than $L - \ell$ away from v can contribute to $\mathbf{h}_{u,v}^{(L)}$ in the ℓ -th step. In this way, we implicitly encode relevant entities and relations in the biomedical network from u to v . We provide a graphical illustration (Supplementary Figure 2) of the implicit encoding procedure as follows.

- When $\ell = 0$, only $\mathbf{h}_{u,u}^0$ is initialized with the non-zero features \mathbf{f}_u (in black) and other entities are initialized as $\mathbf{0}$ (in gray).
- During the ℓ -th iteration, the representations are flowed from u to the ℓ -th hop neighbors of u in the ℓ -th step (like the formulas in black, representing the representing a node in corresponding layer).

- At the last step $\ell = L$, $\mathbf{h}_{u,v}^L$ is used as the subgraph representation. We use boxes to indicate the representations participated in the computation of $\mathbf{h}_{u,v}^L$ in each step.
- As shown, the entities in each step are identical to the entities in the left bottom figure, implicitly encoding the subgraph representation.

Algorithm for path extraction. Given a drug pair (u, v) , we use beam search to find the top $B = 5$ paths in the direction from u to v and top $B = 5$ paths from v to u . Take the direction from u to v as an example. We provide the path extraction procedure in Algorithm 2. We provide three kinds of lists: openList, recording the top K entities in each step; closeList, recording the accumulated scores of entities visited in each step; pathList, recording the searched paths at each step. In lines 3-4, we obtain the sets of entities visited in the ℓ -th step $\mathcal{V}_{u,v}^{(\ell)}$ through bi-directional bread-first-search. For each step, we compute the accumulated scores of entities $e \in \mathcal{V}_{u,v}^\ell$ by summing the attention score $\alpha_r^{(\ell)}$ in lines 7-8, and record the scores to the clostList. Then we pick up edges with top- B scores, and add them to openList and pathList for next step computation in lines 11-13. After L steps, we aggregate the selected paths in pathList[1], ..., pathList[L] to obtain the top- B paths from u to v . The same steps are conducted to obtain the top- B paths from v to u .

Algorithm 2 Path extractor

Require: $(u, v), L, B$ $\{B: \text{the number of top paths in each direction.}\}$

- 1: initialize openList[0] $\leftarrow u$;
- 2: set $\mathcal{V}_{u,v}^{(0)} = \{u\}, \mathcal{V}_{u,v}^{(L)} = \{v\}$;
- 3: obtain the set $\mathcal{V}_{u,v}^{(\ell)} = \{e : d(e, u) = \ell, d(e, v) = L - \ell\}, \ell = 1, \dots, L$ with bread-first-search;
- 4: **for** $\ell \leftarrow 1$ to L **do**
- 5: set closeList[ℓ] $\leftarrow \emptyset$, pathList[ℓ] $\leftarrow \emptyset$;
- 6: **for** each edge in $\{(e', r, e) : e' \in \text{openList}[\ell - 1], e \in \mathcal{V}_{u,v}^\ell\}$ **do**
- 7: compute the attention weights $\alpha_r^{(\ell)}$;
- 8: compute $\text{score}(u, e', e) = \text{score}(u, e) + \alpha_r^{(\ell)}$;
- 9: closeList[ℓ].add($(e, \text{score}(u, e', e))$);
- 10: **end for**
- 11: **for** $(u, e', e) \in \text{top}_B(\text{closeList}[\ell])$ **do**
- 12: openList[ℓ].add(e), pathList[ℓ].add((e', r, e));
- 13: **end for**
- 14: **end for**
- 15: **Return:** join(pathList[1]..pathList[L]).

Comparison of EmerGNN with other deep learning methods for link prediction. The general pipeline for GNN-based link prediction contains three parts: subgraph extraction, node labeling, and GNN learning. Take

SEAL [31] as an example. It firstly extracts enclosing subgraph, which contains the intersection of L -hop neighbors of (u, v) , between drug pairs. In order to distinguish the nodes on the subgraph, SEAL then labels the nodes based on their shortest path distance to both nodes u and v . Finally, a GNN aggregates the representations of node labels for L steps, integrates the representations of all the nodes, and predicts the interaction based on the integrated representation.

On subgraph extraction, we use union of paths to form a path-based subgraph instead of the enclosing subgraph, as we need to integrate the entities and relations on the augmented network while propagating from drug u to v . Node labeling is difficult to be extended to heterogeneous graph, and a simple extension from homogeneous graph may not lead to good performance [32]. In comparison, our designed flow-based GNN avoids the labeling problem by propagating from u to v step-by-step. Benefiting by the propagation manner, we do not need use an extra pooling layer [28, 31, 32] and just use the pair-wise representation $\mathbf{h}_{u,v}^{(L)}$ in the last step to encode the path-based subgraph $\mathcal{G}_{u,v}^L$. The above benefits are demonstrated in Fig. 5c (main text) and we provide more analysis in Supplementary Figure 4.

Supplementary Section 2 Additional Results

Implementation of baselines. We summarize the details of how baseline methods are implemented for the DDI prediction tasks.

- **MLP** [9]. For each drug, there is a fingerprint vector with 1024 dimensions generated based on the drug’s SMILES attributes, which stand for Simplified Molecular Input Line Entry System. Given a pair of drugs u and v , the fingerprints \mathbf{f}_u and \mathbf{f}_v are firstly fed into an MLP with 3 layers, respectively. Then the representations are concatenated to compute the prediction logits with $l(u, v) = \mathbf{W}_{\text{rel}}[\mathbf{h}_{u,v}^{(L)}; \mathbf{h}_{v,u}^{(L)}]$.
- **Similarity** [4]. We generate four fingerprints based on the SMILES representation for each drug. For a given pair of drugs, we compute the similarity features between this drug pair and a known set of DDIs. Specifically, we compare the 16 pairwise similarity features composed of the fingerprints of each drug pair, and select the maximum similarity value as the similarity feature for the current drug pair. Subsequently, we input these features into a random forest model to predict the DDIs.
- **CSMDDI** [11]. CSMDDI uses a RESCAL-based method to obtain embedding representations of drugs and DDI types. It then utilizes partial least squares regression to learn a mapping function to bridge the drug attributes to their embeddings to predict DDIs. Finally, a random forest classifier is trained as the predictor, and the output of the random forest classifier provides the final prediction score for the interaction between two drugs. The implementation follows <https://github.com/itsosy/csmddi>.

- **STNN-DDI** [21]. STNN-DDI learns a substructure \times substructure \times interaction tensor, which characterizes a substructure-substructure interaction (SSI) space, expanded by a series of rank-one tensors. According to a list of predefined substructures with PubChem fingerprint, two given drugs are embedded into this SSI space. A neural network is then constructed to discern the types of interactions triggered by the drugs and the likelihood of triggering a particular type of interaction. The implementation follows <https://github.com/zsy-9/STNN-DDI>.
- **HIN-DDI** [5]. We constructs a heterogeneous information network (HIN) that integrates a biomedical network with DDIs. Within this network, we defined 48 distinct meta-paths, representing sequences of node types (including compounds, genes, and diseases) that connect nodes in the HIN. For each meta-path, a series of topological features, such as path count, was generated. Subsequently, these features were normalized and inputted into a random forest model for DDI prediction.
- **MSTE** [12]. MSTE learns DDI with knowledge graph embedding technique and models the interactions as triplets in the KG. Specifically, for each interaction $(u, i, v) \in \mathcal{N}_D$, there are learnable embedding vectors $e_u, e_v \in \mathbb{R}^d$ for the drugs u and v , respectively, and $i \in \mathbb{R}^d$ for interaction type i . MSTE then computes a score $s(u, i, v) = \|\sin(i \cdot e_v) \cdot e_u + \sin(e_u \cdot e_v) \cdot i - \sin(e_u \cdot i) \cdot e_v\|_{1/2}$, which is then used as a negative logit for the prediction of interaction type i . The dimension d is a hyper-parameter tuned among $\{32, 64, 128\}$. The implementation follows <https://github.com/galaxysunwen/MSTE-master>.
- **KG-DDI** [14]. KG-DDI uses a Conv-LSTM network on top of the embeddings to compute the score of interaction triplets $(u, i, v) \in \mathcal{N}_D$ as well as the biomedical triplets $(h, r, t) \in \mathcal{N}_B$. Different from MSTE, KG-DDI firstly optimizes the parameters on both the interaction triplets and biomedical triplets, namely triplets in the augmented network, then fine-tunes on the interaction triplets for final prediction. The implementation follows <https://github.com/rezacsedu/Drug-Drug-Interaction-Prediction>.
- **CompGCN** [28]. All the drugs, biomedical concepts, interactions and relations have their own learnable embeddings. These embeddings are aggregated by a graph neural network with 1 layer. The high-order embeddings $\mathbf{h}_u^L, \mathbf{h}_v^L, \mathbf{h}_i^L$ are used to compute the score $s(u, i, v) = \langle \mathbf{h}_u^L, \mathbf{h}_v^L, \mathbf{h}_i^L \rangle$, which is then used as the logic of interaction type i . The implementation follows <https://github.com/malllabiisc/CompGCN>.
- **Decagon** [13]. Decagon is similar to CompGCN. The main difference is that the input biomedical network only considers biomedical concepts of drugs, genes and diseases, rather than the full biomedical network \mathcal{N}_B .
- **KGNN** [16]. KGNN is built upon a GNN which propagates information and learns node representations within the new knowledge graph. Considering computational efficiency, KGNN employed neighbor sampling, with four

neighbors sampled per layer for a total of two layers. Subsequently, the learned node representations were used to predict DDIs. The implementation follows <https://github.com/xzenglab/KGNN>.

- **SumGNN** [6]. SumGNN has three steps. First, we extract enclosing subgraphs from the augmented network for all the drug pairs (u, v) to be predicted. Second, a node labeling trick is applied for all the enclosing subgraphs to compute the node features. Then, a graph neural network computes the graph representations of enclosing subgraphs, which are finally used to predict the interaction. The implementation follows <https://github.com/yueyu1030/SumGNN>.
- **DeepLGF** [17]. The DeepLGF model contains three parts. First, the SMILES of drugs are used as sentences to encode the drugs’ chemical structure. Second, a KG embedding model ComplEx is applied on the biomedical network to get the global embedding information of drugs. Third, a relational-GNN is used to aggregate the representations from the biomedical network. Finally, the three kinds of representations are fused with an MLP module for the DDI prediction. Since there is no official code provided, we implement this model based on CompGCN.

Performance comparison of the S0 setting. There are three basic settings for the DDI prediction [10, 11, 21]: (S0) interaction between existing drugs; (S1) interaction between emerging and existing drugs; and (S2) interaction between emerging drugs.

EmerGNN has shown substantial advantage over the baseline methods for emerging drug prediction in Table 1 (main text). We also compare the performance in the S0 setting for prediction between existing drugs in Supplementary Table 3, where the setting exactly follows [6]. Comparing the two tables, we find that the emerging drug prediction task is much harder than existing drug prediction as the accuracy values in the Table 1 (main text) are much lower than those in Supplementary Table 3. Even though the shallow models MLP, **Similarity**, **HIN-DDI** perform well in predicting DDIs for emerging drugs, they are worse than the deep networks when predicting DDIs between existing drugs. The embedding model **MSTE** performs very poorly for emerging drugs but is the third best for existing drug prediction. The GNN-based methods, especially **SumGNN**, also works well for predicting DDIs between existing drugs. This demonstrates that drug embeddings and deep networks can be helpful for drug interaction prediction if sufficient data are provided. **EmerGNN**, even though specially designed for emerging drug prediction, still outperforms the baselines with a large margin for predicting interactions between existing drugs. These results again show the flexibility and strengths of **EmerGNN** on the DDI prediction task.

Path visualization. We provide additional results for path visualization between the case of S1 setting and S0 setting (Supplementary Figure 5).

Specifically, we choose examples with predicted interaction types #52, #5 and #18 in Supplementary Table 5. We plot the interactions between emerging and existing drugs in the left part, and the interactions between two existing drugs in the right part. As shown in Supplementary Figure 5, relation type CrC plays an important role during prediction, which is also reflected by the high correlations in Fig. 3c (main text). For the interaction types on the subgraphs, we also observe the correlations of interaction types, namely (#52, #39), (#5, #85) and (#18, #49), which are identified in Supplementary Table 5. Comparing the left part with right part, we observe that the biomedical entities, like Gene::1565, Disease::DOID:10763 and Pharmacologic Class::N000000102(9), play the role to connect the emerging drug and existing drug. However, the prediction of interactions between two existing drugs relies mainly on the DDI between drugs. These results again verify the claim that EmerGNN is able to identify and leverage the relevant entities and relations in the biomedical network.

Supplementary Tables

Supplementary Table 1: Statistics of datasets used for predicting interactions for DDI prediction. \mathcal{V} 's represent the sets of nodes. \mathcal{R} 's represent the sets of interaction types. \mathcal{N} 's represent the sets of edges.

S0 setting: prediction interactions between exiting drugs.

Statistics	$ \mathcal{V}_D $	$ \mathcal{R}_I $	$ \mathcal{N}_{D\text{-train}} $	$ \mathcal{N}_{D\text{-valid}} $	$ \mathcal{N}_{D\text{-test}} $
Drugbank	1,710	86	134,641	19,224	38,419
TWOSIDES	604	200	177,568	24,887	49,656

S1 and S2 settings: predicting interactions for emerging drugs.

Data	seed	$ \mathcal{V}_{D\text{-train}} $	$ \mathcal{V}_{D\text{-valid}} $	$ \mathcal{V}_{D\text{-test}} $	$ \mathcal{R}_I $	$ \mathcal{N}_{D\text{-train}} $	S1		S2	
							$ \mathcal{N}_{D\text{-valid}} $	$ \mathcal{N}_{D\text{-test}} $	$ \mathcal{N}_{D\text{-valid}} $	$ \mathcal{N}_{D\text{-test}} $
DrugBank	1	1,461	79	161	86	137,864	17,591	32,322	536	1,901
	12	1,465	79	161	86	140,085	17,403	30,731	522	1,609
	123	1,466	81	161	86	140,353	14,933	32,845	396	1,964
	1234	1,463	81	162	86	139,141	15,635	33,254	434	1,956
	12345	1,461	80	169	86	133,394	17,784	35,803	546	2,355
TWOSIDES	1	514	30	60	200	185,673	16,113	45,365	467	2,466
	12	514	30	60	200	172,351	23,815	48,638	717	3,373
	123	514	30	60	200	181,257	18,209	46,969	358	2,977
	1234	514	30	60	200	186,104	25,830	35,302	837	1,605
	12345	514	30	60	200	179,993	22,059	43,867	702	2,695

Biomedical network: HetioNet [18] is used in this paper.

Data	Seed	$ \mathcal{V}_B $	$ \mathcal{R}_B $	$ \mathcal{N}_B $	$ \mathcal{N}_{B\text{-train}} $	$ \mathcal{N}_{B\text{-valid}} $	$ \mathcal{N}_{B\text{-test}} $
DrugBank	1	34,124	23	1,690,693	1,656,037	1,666,317	1,690,693
	12	34,124	23	1,690,693	1,658,075	1,668,273	1,690,693
	123	34,124	23	1,690,693	1,657,489	1,667,685	1,690,693
	1234	34,124	23	1,690,693	1,657,400	1,668,685	1,690,693
	12345	34,124	23	1,690,693	1,656,603	1,668,091	1,690,693
TWOSIDES	1	34,124	23	1,690,693	1,671,519	1,678,548	1,690,693
	12	34,124	23	1,690,693	1,669,693	1,676,696	1,690,693
	123	34,124	23	1,690,693	1,672,632	1,678,335	1,690,693
	1234	34,124	23	1,690,693	1,671,617	1,678,528	1,690,693
	12345	34,124	23	1,690,693	1,672,288	1,678,776	1,690,693

Supplementary Table 2: Hyper-parameters and their tuning ranges for hyper-parameter selection. For all the baselines and the proposed EmerGNN, we use the hyper-parameter optimization toolbox hyperopt [38] to search for the optimum among 360 of hyper-parameter configurations. The objective of hyper-parameter selection is to maximize the premier metric performance (F1-score in DrugBank and PR-AUC in TWOSIDES) on the validation data. Adam [34] is used as the optimizer to update the model parameters of EmerGNN.

Hyper-parameter	Ranges
Learning rate	$\{1 \times 10^{-4}, 3 \times 10^{-4}, 1 \times 10^{-3}, 3 \times 10^{-3}, 1 \times 10^{-2}\}$
Weight decay rate	$\{1 \times 10^{-8}, 1 \times 10^{-6}, 1 \times 10^{-4}, 1 \times 10^{-2}\}$
Mini-batch size	{32, 64, 128}
Representation size d	{32, 64}
Length of subgraphs L	{2, 3, 4}

Supplementary Table 3: Comparison of different methods on the DDI prediction between two existing drugs (S0 Setting). “DF” is short for “Drug Feature”; “GF” is short for “Graph Feature”; “Emb” is short for “Embedding”; and “GNN” is short for “Graph Neural Network”.

¹

Datasets (S0 setting)		DrugBank			TWOSIDES		
Type	Methods	F1-Score	Accuracy	Kappa	PR-AUC	ROC-AUC	Accuracy
DF	MLP [9]	61.1±0.4	82.1±0.3	80.5±0.2	81.2±0.1	82.6±0.3	73.5±0.3
	Similarity [4]	55.0±0.3	62.8±0.1	67.6±0.1	59.5±0.0	59.8±0.0	57.0±0.1
GF	HIN-DDI [5]	46.1±0.5	54.4±0.1	63.4±0.1	83.5±0.2	87.7±0.3	82.4±0.3
Emb	MSTE [12]	83.0±1.3	85.4±0.7	82.8±0.8	90.2±0.1	91.3±0.1	84.1±0.1
	KG-DDI [14]	52.2±1.1	61.5±2.8	55.9±2.8	88.2±0.1	90.7±0.1	83.5±0.1
GNN	CompGCN [28]	74.3±1.2	78.8±0.9	75.0±1.1	90.6±0.3	92.3±0.3	84.8±0.3
	Decagon [13]	57.4±0.3	87.2±0.3	86.1±0.1	90.6±0.1	91.7±0.1	82.1±0.5
	KGNN [16]	74.0±0.1	90.9±0.2	89.6±0.2	90.8±0.2	92.8±0.1	86.1±0.1
	SumGNN [6]	86.9±0.4	92.7±0.1	90.7±0.1	93.4±0.1	94.9±0.2	88.8±0.2
	EmerGNN	94.4±0.7	97.5±0.1	96.6±0.8	97.6±0.1	98.1±0.1	93.8±0.2
p-values		4.5E-7	6.5E-13	6.7E-8	2.3E-8	5.1E-10	6.1E-7

¹All of the methods are run for five times on the five-fold datasets with mean value and standard deviation reported on the testing data. The evaluation metrics are presented in percentage (%) with the larger value indicating better performance. The boldface numbers indicate the best values, while the underlined numbers indicate the second best. p-values are computed under two-sided t-testing of EmerGNN over the second best baselines.

Supplementary Table 4: Complexity analysis of different GNN-based methods in the S1 setting in terms of GPU memory footprint and the number of model parameters.

	DrugBank		TWOSIDES	
	GPU memory (MB)	Model parameters	GPU memory (MB)	Model parameters
Decagon	8,214	1,766,492	2,908	1,145,850
SumGNN	6,968	1,237,628	12,752	1,263,188
DeepLGF	16,822	11,160,226	5,974	10,012,456
EmerGNN	7,104	137,164	2,040	156,406

Supplementary Table 5: Detailed explanation on the highlighted interaction pairs (three yellow circles) in Fig. 3a (main text). The interaction IDs are from the original DrugBank datasets.

ID	Description	Exemplar drug-pairs
#52	#Drug1 may decrease the analgesic activities of #Drug2.	(Tapentadol, Dolasetron)
#39	#Drug1 may increase the constipating activities of #Drug2.	(Cyclopentolate, Ramosetron)
Evidence	Oral naloxone is efficacious in reversing opioid-induced constipation, but often causes the unwanted side effect of analgesia reversal [26].	
#5	#Drug1 may decrease the vasoconstricting activities of #Drug2.	(Labetalol, Formoterol)
#85	#Drug1 may increase the tachycardic activities of #Drug2.	(Duloxetine, Droxidopa)
Evidence	This decrease in afferent signaling from the baroreceptor causes vasoconstriction and increased heart rate (tachycardic) [39].	
#18	#Drug1 can cause an increase in the absorption of #Drug2 resulting in an increased serum concentration and potentially a worsening of adverse effects.	(Ethanol, Levomilnacipran)
#49	The risk or severity of adverse effects can be increased when #Drug1 is combined with #Drug2.	(Methyl salicylate, Triamcinolone)
Evidence	Both of the two interactions are related to worsening adverse effects when two drugs are combined together.	

Supplementary Table 6: Detailed explanation of selected paths from the learned model. In these cases, we provide the target interaction sample to be predicted, two important paths selected by our method, and the corresponding explanations.

Case 1 in Fig. 4a.

Target: Tapentadol (DB06204) may decrease the analgesic activity of Dolasetron (DB00757).

Path1 (0.6666): Tapentadol $\xrightarrow{\text{binds}}$ CYP2D6 (P450) $\xrightarrow{\text{binds.inv}}$ Dolasetron

Explanation: Tapentadol can binds the P450 enzyme CYP2D6 (Gene::1565), which is vital for the metabolism of many drugs like Dolasetron (Estabrook, 2003). In addition, Binding of drug to plasma proteins is reversible, and changes in the ratio of bound to unbound drug may lead to drug-drug interactions (Kneip et. al. 2008).

Path2 (0.8977): Dolasetron $\xrightarrow{\text{resembles}}$ Hyoscyamine $\xrightarrow{\#39:\uparrow\text{constipating}}$ Eluxadoline $\xrightarrow{\#39.inv}$ Tapentadol

Explanation: Dolasetron is similar to drug Hyoscyamine (DB00424). Hyoscyamine and Tapentadol can get some connection since they will both increase the constipating activity of Eluxadoline (DB09272). As suggested by Liu and Wittbrodt (2022), reversing opioid-induced constipation often causes the unwanted side effect of analgesia reversal.

Case 2 in Fig. 4a.

Target: Labetalol (DB00598) may decrease the vasoconstricting activity of Metaraminol (DB00610).

Path1 (0.8274): Labetalol $\xrightarrow{\text{resembles}}$ Isoxsuprine $\xrightarrow{\#8.inv}$ Dronabinol $\xrightarrow{\#85:\uparrow\text{tachycardic}}$ Metaraminol

Explanation: Labetalol is similar to the drug Isoxsupirune (DB08941). Isoxsupirune and Metaraminol can get some connection since Dronabinol (DB00470) will increase the tachycardic activity of both of them. As suggested by Chaudhry et al (2022), the decrease of vasoconstriction and the increase of tachycardic are often correlated.

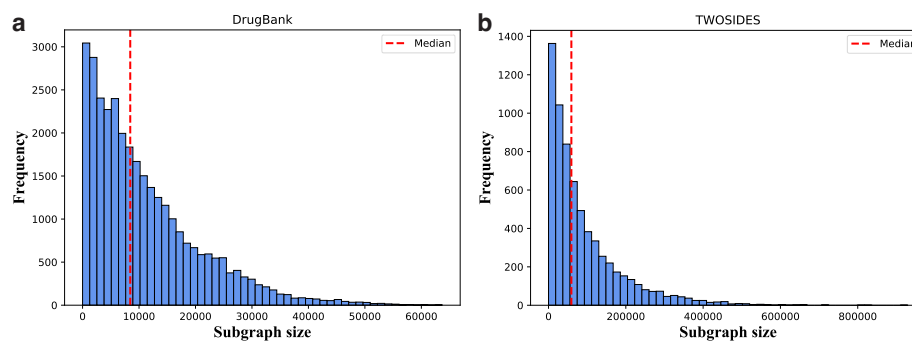
Path2 (0.8175): Metaraminol $\xrightarrow{\#5:\downarrow\text{vasoconstricting.inv}}$ Spironolactone $\xrightarrow{\text{treat}}$ hypertension $\xrightarrow{\text{treat.inv}}$ Labetalol

Explanation: Labetelol and Spironolactone (DB00421) get can some connections since they treat the same disease hypertension (DOID:10763). As Spironolactone may decrease the vasoconstricting activity of Metaraminol (indicated by the inverse edge), we predict that Labetelol may also decrease the vasoconstricting activity of Metaraminol.

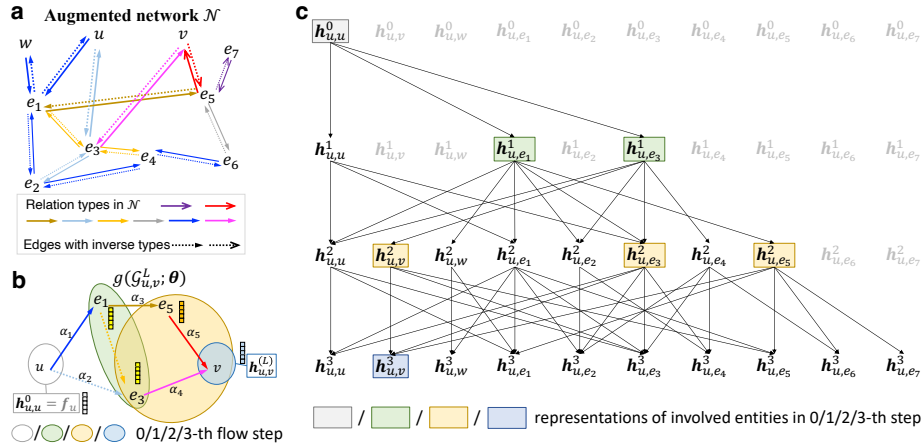
Supplementary Table 7: Performance comparison of different technique designing in EmerGNN on DrugBank dataset. “Undirected edges w.o. inverse” means the variant that uses undirected edges instead of introducing the inverse edges. “Subgraph representation” means the variant that learns a subgraph representation as SumGNN upon $\mathcal{G}_{u,v}^L$. “Uni-directional pair-wise representation” means the variant that only learns on the uni-directional computing (Method) from direction u to v without considering the direction from v to u . The performance of EmerGNN is provided in the last row as a reference.

Variants of designing	F1-Score	Accuracy	Kappa
Undirected edges w.o. inverse	53.7±2.0	61.8±1.9	54.8±2.0
Subgraph representation	33.1±3.6	50.2±5.6	40.7±5.6
Uni-directional pair-wise representation	55.6±2.1	67.4±1.6	61.1±1.6
EmerGNN	62.0±2.0	68.6±3.7	62.4±4.3

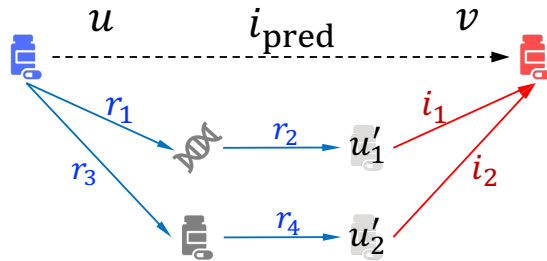
Supplementary Figures



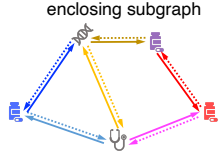
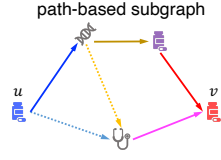
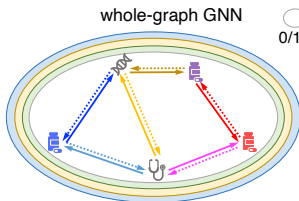
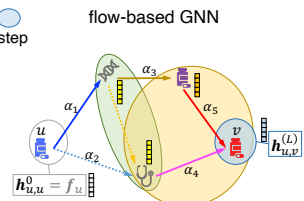
Supplementary Figure 1: Histograms of subgraph sizes of $\mathcal{G}_{u,v}^L$ (indicated by the number of edges) in the testing sets of two datasets when $L = 3$. Median values (8,444 for DrugBank and 59,120 for TWOSIDES) are indicated by the red dashed line.



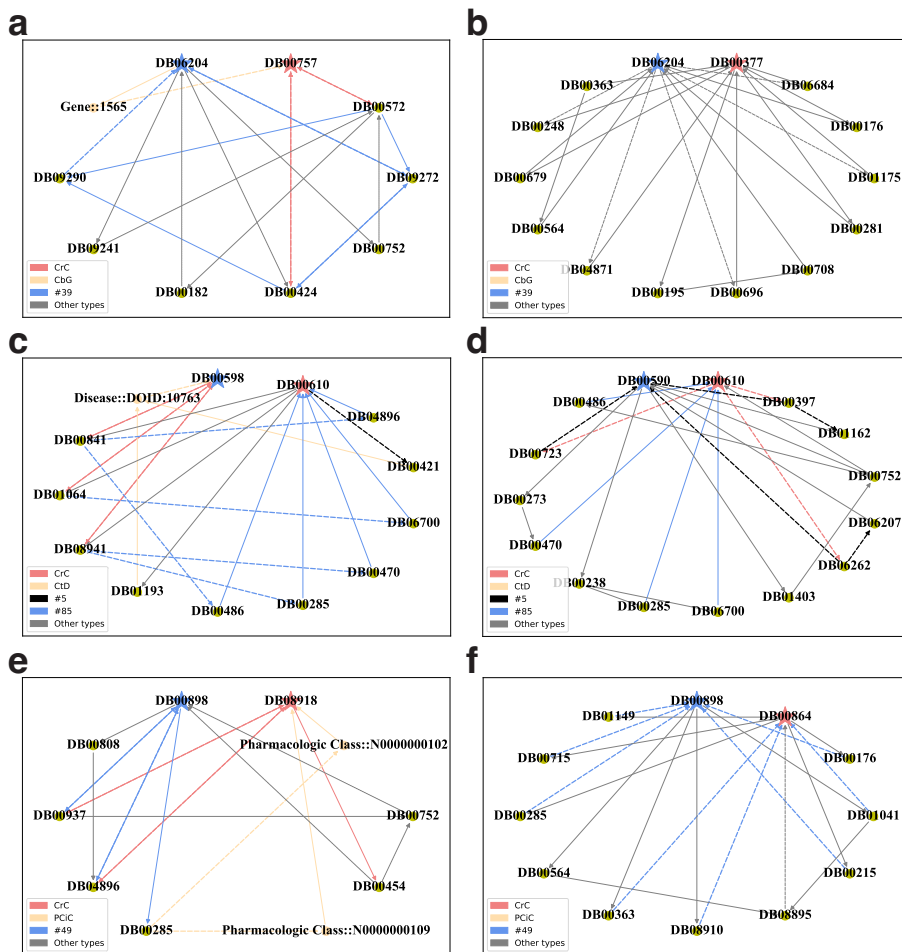
Supplementary Figure 2: A graphical illustration of why the initialization step together with the message propagation function can implicitly encode the visible entities in each layer (step ℓ). **(a)** Symbolic representation of the augmented network in the example of Fig. 1 (main text). Different colors in edges mean different relation types (in Fig. 1a) and the dashed lines mean the inverse edges with corresponding relation type. **(b)** Symbolic representation of the flow-based GNN from u to v . The four circles in different colors indicate the involved entities in different steps. **(c)** Representation flows according to the proposed Algorithm 1 (gray symbols mean $\mathbf{0}$ vectors, and the relation types in lines are omitted for simplicity). From top to bottom, we show how the representations are activated and propagated in each step. The involved entities in each step in (b) and (c) are identical to each other, indicating that our algorithm can implicitly encoding the subgraph representation.



Supplementary Figure 3: A graphical exemplar of selected paths (the different icons mean different drugs and genes). We show how the correlation matrices in Fig. 3a and 3c (main text) are calculated based on this example. Given the interaction triplet (u, i_{pred}, v) to be predicted, we extract several paths (two in this figure) through Algorithm 2. Here, we have two paths which contain some relations $\{r_1, \dots, r_4\}$ in the biomedical network \mathcal{N}_B and interactions $\{i_1, i_2\}$ in the interaction network \mathcal{N}_D . The co-occurrence times for each type $i \in \mathcal{R}_I$ and $r \in \mathcal{R}_B$ are counted on the paths for different interaction triplets. For the interaction types $i \in \mathcal{R}_I$ or biomedical relation types $r \in \mathcal{R}_B$, we group their counting values according to the to-be-predicted interaction i_{pred} and normalize the values by dividing the frequency of i_{pred} in $\mathcal{N}_{D\text{-test}}$.

Subgraph		
Node labeling	needed	not needed
GNN architecture		
Pooling	Representations of all the entities in subgraph $\{h_e^{(L)}, e \in \mathcal{V}_{u,v}^L\}$ are pooled for prediction	$\mathbf{h}_{u,v}^{(L)}$ is directly used for prediction

Supplementary Figure 4: A detailed comparison between SumGNN and EmerGNN in terms of subgraph structure, usage of node labeling, GNN architecture design and the pooling mechanism. Different colors in the edges indicate different relation types. The different circles mean different computing steps in GNNs. **Subgraph**: The enclosing subgraph used in SumGNN contains all the edges among entities within L steps away from both u and v ; the path-based subgraph only considers edges pointing from u to v or v to u . **Node labeling**: SumGNN requires a node labeling procedure to compute the distance of nodes on the subgraph to the target drugs u and v ; however, as the edges are connected in the direction from u to v , in EmerGNN, the distance information can be reflected by the number of jumps, thus EmerGNN does not need a node labeling procedure. **GNN architecture**: SumGNN uses the whole-graph GNN as in [31, 32, 40] to propagate over the whole subgraph. EmerGNN uses the flow-based GNN to propagate information from u to v step-by-step with a better control of information flow. **Pooling**: In SumGNN, the representations of all the entities in the subgraph should be pooled (for example concatenated) for final interaction prediction; however, benefiting from the flowing pattern of flow-based GNN, all the information can be ordered and integrated when propagating from u to v , thus EmerGNN only uses the final step representation of v , namely $\mathbf{h}_{u,v}^{(L)}$, for interaction prediction.



Supplementary Figure 5: Visualization of learned paths between drug pairs. Left: interactions between an existing drug and an emerging drug. Right: interactions between two existing drugs. The dashed lines mean inverse types. (a,b) DB00757 (Dolasetron) is an emerging drug. DB06204 (Tapentadol) and DB00377 (Palonosetron) are existing drugs. The prediction interaction type is #52 (#Drug1 may decrease the analgesic activities of #Drug2.). (c,d) DB00598 (Labetalol) is an emerging drug. DB00610 (Metaraminol) and DB00590 (Doxazosin) are existing drugs. The prediction interaction type is #5 (#Drug1 may decrease the vasoconstricting activities of #Drug2.). (e,f) DB08918 (Levomilnacipran) is an emerging drug. DB00898 (Ethanol) and DB00864 (Tacrolimus) are existing drugs. The prediction interaction type is #18 (#Drug1 can cause an increase in the absorption of #Drug2 resulting in an increased serum concentration and potentially a worsening of adverse effects.).